



ELSEVIER

Clinical Neurology and Neurosurgery xxx (2005) xxx–xxx

**Clinical Neurology
and Neurosurgery**

www.elsevier.com/locate/clineneuro

Case report

Respiratory failure in a patient with antecedent poliomyelitis: Amyotrophic lateral sclerosis or post-polio syndrome?

Shin-ichi Terao^{a,b,*}, Naofumi Miura^a, Aiji Noda^a,
Mari Yoshida^b, Yoshio Hashizume^b, Hiroshi Ikeda^c, Gen Sobue^d

^a Division of General Medicine, Department of Internal Medicine,
Aichi Medical University School of Medicine, Aichi 480-1195, Japan

^b Institute for Medical Science of Aging, Aichi Medical University School of Medicine, Japan

^c Department of Pathology, Aichi Medical University School of Medicine, Japan

^d Department of Neurology, Nagoya University, Graduate School of Medicine, Japan

Received 29 October 2004; received in revised form 9 March 2005; accepted 13 March 2005

Abstract

We report a 69-year-old man who developed paralytic poliomyelitis in childhood and then decades later suffered from fatal respiratory failure. Six months before this event, he had progressive weight loss and shortness of breath. He had severe muscular atrophy of the entire right leg as a sequela of the paralytic poliomyelitis. He showed mild weakness of the facial muscle and tongue, dysarthria, and severe muscle atrophy from the neck to proximal upper extremities and trunk, but no obvious pyramidal signs. Electromyogram revealed neurogenic changes in the right leg, and in the paraspinal, sternocleidomastoid, and lingual muscles. There was a slight increase in central motor conduction time from the motor cortex to the lumbar anterior horn. Pulmonary function showed restrictive ventilation dysfunction, which was the eventual cause of death. Some neuropathological features were suggestive of amyotrophic lateral sclerosis (ALS), namely Bunina bodies. In patients with a history of paralytic poliomyelitis who present after a long stable period with advanced fatal respiratory failure, one may consider not only respiratory impairment from post-polio syndrome but also the onset of ALS.

© 2005 Elsevier B.V. All rights reserved.

Keywords: Motor neuron disease; Neuropathological study; Postmortem study; Pulmonary functions

1. Introduction

Amyotrophic lateral sclerosis (ALS) is a neurodegenerative disease with selective and systematic involvement of the cortical and spinal motor neurons, causing systemic muscle atrophy including of the respiratory muscle [1–6]. Acute paralytic poliomyelitis is caused by infection with the poliovirus in childhood, which produces spinal motor neuron damage. This disease affects mainly the proximal muscles of the legs, and leads to asymmetric flaccid paralysis and atrophy. With the spread of the polio vaccine in the modern

era, poliomyelitis has become uncommon. However, in acute paralytic poliomyelitis patients, various functional disorders sometimes appear decades after the initial disease. These disorders exacerbate motor, sensory, and respiratory dysfunction and are known collectively as post-polio syndrome (PPS) or post-polio muscular atrophy (PPMA) [7–10], which often mimics ALS symptoms. Conversely, ALS is rarely associated with antecedent paralytic polio, and mimics PPS [11–13]. About 1% of paralytic polio patients have been reported to develop ALS [14]. This rate is extremely high compared with the general prevalence of ALS. It is not yet clear whether the development of ALS is linked to paralytic polio [15–17].

We report a patient with severe residual paralysis in one leg from paralytic polio in childhood, who suffered fatal respiratory impairment in old age.

* Corresponding author at: Department of Neurology, Nagoya Ekisaiikai Hospital, Nagoya, Aichi 454-0854, Japan. Tel.: +81 52 652 7711; fax: +81 52 652 7783.

E-mail address: terao123@quartz.ocn.ne.jp (S.-i. Terao).

2. Case report

The patient was a 69-year-old man. His history included febrile-associated acute motor palsy at the age of 4 years, and subsequent muscle atrophy and right leg paralysis. These conditions were arrested after the initial disease, with no relapse or progression. Other limb weakness and atrophy was not present. This clinical history strongly suggests that the patient suffered from poliomyelitis. His early acute anterior poliomyelitis did not seem to involve respiratory muscles. At 20 years of age his right upper lung was partially resected because of tuberculosis. He had a 40-year history of smoking. There was no history of neuromuscular disease in his family.

For 6 months before presentation, the patient had gradually progressing loss of weight and appetite, and noticed shortness of breath upon walking or exertion. For 3 months, he had gradually progressing general malaise, difficulty speaking, and a weak voice. He had difficulty in sleeping, but no snoring or apnea during sleep. He lost 10kg in weight in 6 months, and visited our hospital because of breathing difficulty.

At the initial examination, he was alert and intelligent. His height was 158 cm, weight 37 kg, blood pressure 100/70 mmHg, body temperature 36.7°C, and pulse rate 62 beats/min. He had no arrhythmia. Movement of the thorax was extremely limited on breathing. Severe muscle atrophy was seen from the right hip through the entire leg, and the right leg was 5 cm shorter than the left. There was mild weakness in the facial muscles, dysarthria, and mild paralysis and fasciculation of the tongue, but no dysphagia. Muscles from

the neck through the proximal arms and trunk were severely atrophied, but there was no fasciculation. Grip strength was 27 kg in the right hand and 25 kg in the left. Limb weakness was minimal except for the right leg. Deep tendon reflexes in the limbs were decreased overall. Neither spasticity nor Babinski's sign were present. He had no sensory impairment.

Blood tests revealed no anemia, and there were no abnormalities in biochemical test results. Thyroid function was normal, but tests were positive for HBs antigen and HCV antibody. There were no findings of pneumonia on chest radiograph, and no paresis of the diaphragm. Arterial blood gas analysis (room air) findings were PH 7.368, PaO₂ 89.8 Torr, PaCO₂ 59.2 Torr, HCO₃ 33.3 mEq/L, and SaO₂ 97.0%. There were no abnormalities on electrocardiogram. Clinical respiratory symptoms showed no improvement with edrophonium. Motor, sensory and F-wave conduction velocities in the limbs were all within the normal range. Electromyogram revealed marked neurogenic changes in the right quadriceps femoris and tibialis anterior muscles. In addition, polyphasic and high amplitude potentials were observed in the paraspinal, sternocleidomastoid and lingual muscles. Repetitive stimulation was not performed with this patient. Measurement of central motor conduction was done using the technique of percutaneous magnetic stimulation of the brain and spinal cord. Central motor conduction time from the cerebral motor cortex to the cervical segment of the spinal cord (C-CMCT) was measured by subtracting the latency to onset of EMG activity of the thenar muscle after cervical stimulation from the latency to onset of EMG activity to the same muscle after scalp stimulation. The latencies to onset of the action potential of the

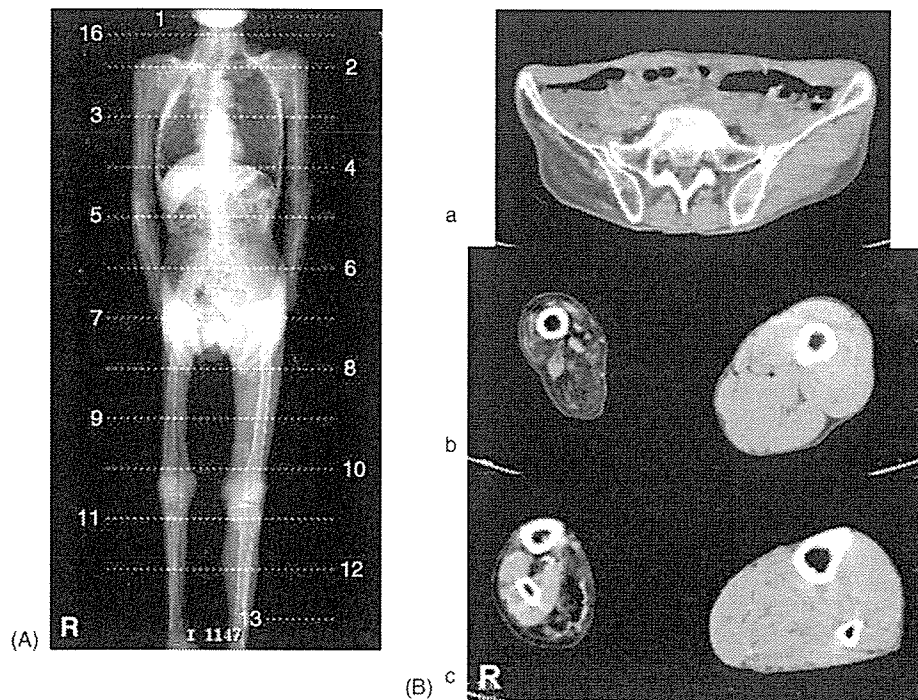


Fig. 1. CT findings. (A) Shows a full body image. (B) Shows transverse sections at the levels of the inferior pelvis (a), mid-thigh (b), and mid-calf (c). The right leg is shorter. Severe atrophy and fatty degeneration are seen from the right hip through the leg.

abductor hallucis muscle after scalp stimulation and to onset of the action potential of the same muscle after lumbar stimulation were also measured, and the difference between the two latencies was estimated as central motor conduction time from the cortex to the lumbar segment of the spinal cord (L-CMCT). The C-CMCT for the right thenar muscle was 9.4 ms (normal: up to 10 ms). The L-CMCT for the abductor hallucis muscle was 15.8 ms, showing a slight increase (normal: up to 15 ms). On spirometry, forced vital capacity (FVC) was 1.87 L, % predicted value (%VC) was 59.8%, and forced expiratory volume (FEV) 1.0% was 81.7%, showing restrictive ventilation dysfunction. There were no abnormalities in cerebrospinal fluid, which tested negative for type I poliovirus antibodies. CT showed diffuse severe muscular atrophy and fatty degeneration from the right hip through the entire leg (Fig. 1A and B). Atrophy of the paraspinal and intercostal muscles was also seen. Brain MRI showed mild atrophy, but no abnormal signals were seen along the corticospinal tract.

Two months after admission he required non-invasive positive pressure ventilation by nasal mask for his sleep disorder. After 4 months he could not orally ingest food sufficiently because of his breathing difficulty. After 5 months his pulmonary function showed an FVC of 0.99 L, %VC of 38.1%, and FEV 1.0% of 41.3%. In arterial blood gas analysis (room air), both PaO₂ and PaCO₂ continued to be about 60 Torr. After 6 months the patient died from respiratory failure. The clinical diagnosis was a residue of paralytic polio and ALS presenting as respiratory failure. An autopsy was performed about 8 h after death.

Brain weight was 1370 g. No marked changes were seen in the brain grossly, but there was atrophy of the spinal ventral roots. Histologically, motor neuron loss in the spinal ventral horn was seen. In the anterior horn of the left lumbar cord, active degeneration was seen, including atrophied motor neurons with Bunina bodies, appearance of macrophages, axonal spheroids, and hypertrophic astrocytes (Figs. 2–4). On the right side, atrophy of the ventral horn, extensive neuronal loss, and gliosis were seen, but there were few findings of active degeneration (Fig. 3). At the cervical and thoracic levels, there was not a clear difference between motor neuron lesions on the right and left sides. Mild cell loss in the hypoglossal nuclei was present. Bunina bodies were also seen in remaining motor neurons of the cervical anterior horn and the hypoglossal nuclei. There was mild loss of Betz cells in the motor cortex. In the spinal cord, the lateral column demonstrated a slight pallor bilaterally with Klüver–Barrera stain (Fig. 2), and the presence of macrophages. Glial bundles were seen on the right side, particularly in the lumbar ventral roots. Neurogenic atrophy was also seen in the intercostal muscles and diaphragm.

3. Discussion

The present patient had a history of paralytic polio in childhood. After a stable period of about 65 years, he suffered

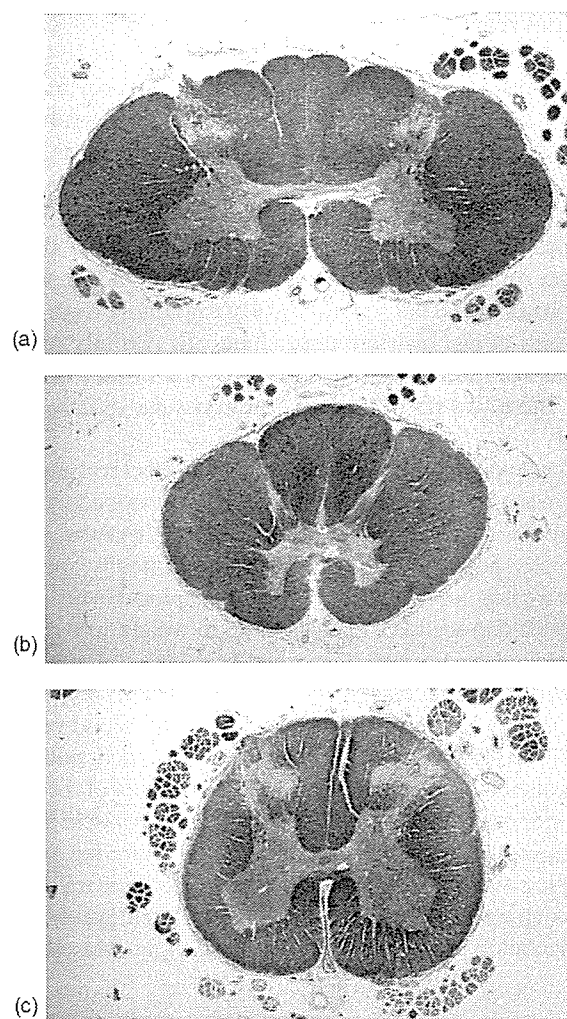


Fig. 2. Spinal cord findings. Transverse section at the spinal level ((a) cervical, (b) thoracic, and (c) lumbar). Mild pallor is seen in the lateral columns at the lumbar level. Klüver–Barrera stain ($\times 3$).

severe weight loss and a respiratory disorder. This was a rare case in which the lower motor neuron symptoms and signs were in the foreground, and the condition rapidly progressed to fatal respiratory failure. The findings included some atypical features for ALS, namely, absence of the obvious clinical pyramidal signs.

Typical symptoms of PPS and PPMA include new deterioration of muscle strength, general fatigue, speech and vocal impairment, dysphagia, and depression.

Rather than a reinfection or reactivation of the poliovirus or a new progressive degenerative process, PPS may be a secondary functional disorder from the addition of age-related changes to existing functional failure [7–10]. Among PPS cases, progressive ventilation failure such as chronic alveolar hypoventilation, progressive respiratory failure, and sleep apnea syndrome have been reported [18,19]. The clinicopathological diagnosis of our patient was more likely ALS presenting as respiratory failure or dyspnea-fasciculation syndrome [20], rather than respiratory disorder due to PPS or PPMA.

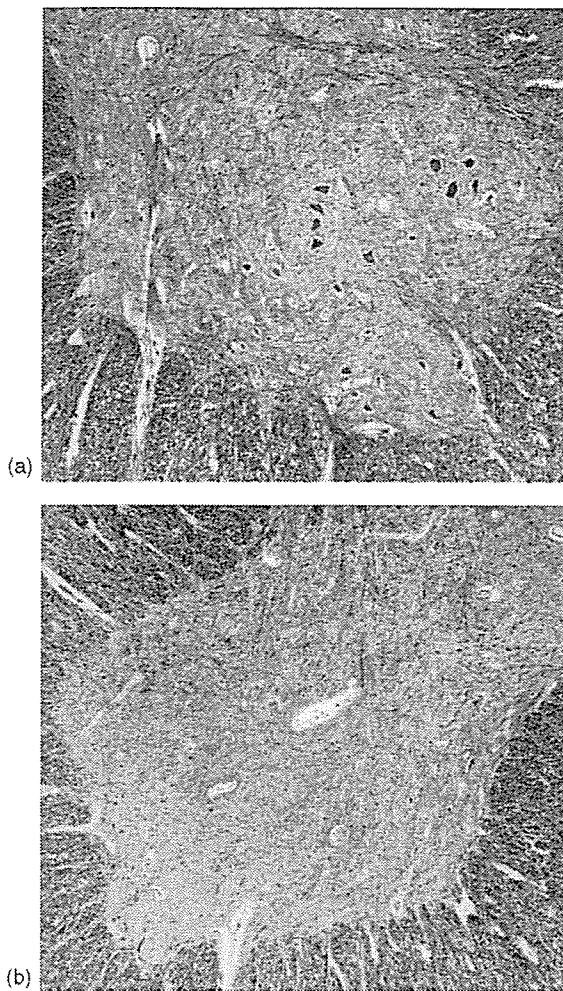


Fig. 3. Spinal ventral horn findings. Transverse sections of the lumbar ventral horn. Mild to moderate loss of motor neurons is seen on the left side (a). On the right side (b), ventral horn atrophy, severe motor neuron loss, and gliosis are seen. Klüver-Barrera stain ($\times 10$).

Recently, Truffert et al. [21] have reported that a 56-year-old man with prior paralytic poliomyelitis developed progressive respiratory failure caused by endplate dysfunction. Repetitive stimulation studies showed a marked decrease

of the trapezius muscle response, which was reversible with edrophonium. In the absence of biological evidence for autoimmune myasthenia gravis, it may be that some kind of endplate dysfunction mechanism is related to postpolio syndrome. The repetitive stimulation procedure should be considered in postpolio syndrome patients as some of them may benefit from anticholinesterase treatment. In our patient the negative result from the edrophonium test was rather unsuggestive of significant endplate dysfunction. Truffert et al. reported a patient whose presentation was quite similar to the present case, but who improved with anticholinesterase therapy, contrary to our patient.

Neuropathological reports on ALS patients with antecedent paralytic polio are rare. Roos et al. [12] reported an ALS patient who had contracted poliomyelitis at the age of 15 years. This patient had weakness of the right hand at the age of 45, and died 3 years later. These authors noted that, neuropathologically, this case presented a classical picture of ALS. Shimada et al. [13] reported a woman who had leg paralysis from acute poliomyelitis at the age of 2 years, onset of progressive weakness of the left hand at the age of 75, and respiratory failure causing death at the age of 80.

Neuropathologically, there were findings of old poliomyelitis in the lumbar ventral horn, together with ALS pathology presenting cortical and spinal motor neuron damage. However, they described several atypical findings that differed from classical ALS [22], including the preservation of the hypoglossal nucleus, no Bunina bodies in the remaining motor neurons, and no ubiquitin-positive inclusions. Pezeshkpour et al. [23] reported local, asymmetric spinal anterior horn motor neuron degeneration and a well-preserved corticospinal tract. Miller [24] indicated that PPMA patients presented spinal motor neuron loss and axon spheroids, and mild spinal lateral funiculus damage and loss of Betz cells in the motor cortex.

In the present case, there was atrophy in the right lumbar anterior horn, and severe loss of cells of all sizes, from large alpha motor neurons to small interneurons. This was quite different from the size-dependent selective pattern of

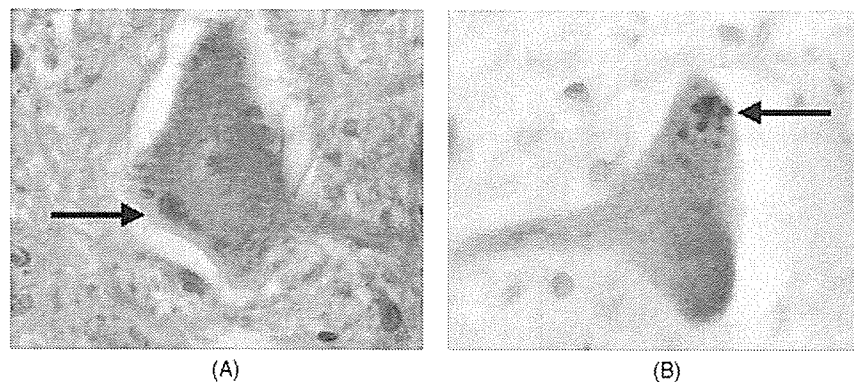


Fig. 4. Bunina body findings. (A) Shows Bunina bodies (arrows) in motor neurons of the lumbar ventral horn with hematoxylin-eosin stain ($\times 100$). (B) Shows cystatin-C stain ($\times 100$).

motor neuron loss in ALS [25–28]. The glial bundles present predominantly in the right lumbar spinal roots were those from paralytic polio [29]. Otherwise, the pathophysiological findings were indistinguishable from those of sporadic ALS. The extremely rapid progression of motor neuron dysfunction resulting in respiratory failure may reflect the underlying dormant pathophysiological process due to antecedent poliovirus infection, since antecedent poliovirus infection would have spread far beyond the lesions of apparent motor neuron loss [18,19].

In patients with a history of paralytic poliomyelitis who present progressive respiratory failure after a long and stable course, one may consider not only respiratory disorder due to PPS but also, in rare cases, the development of ALS.

References

- [1] Bonduelle M. Amyotrophic lateral sclerosis. In: Vinken PJ, Bruyn GW, editors. *System disorders and atrophies. Part II. Handbook of clinical neurology*, vol. 22. Amsterdam: North-Holland Publishing Co.; 1975. p. 281–338.
- [2] Hughes JT. Pathology of amyotrophic lateral sclerosis. *Adv Neurol* 1982;36:61–74.
- [3] Leigh PN, Ray-Chaudhuri K. Motor neuron disease. *J Neurol Neurosurg Psychiatry* 1994;57:886–96.
- [4] Pouget J, Azulay J-P, Bille-Turc F, Sangla I, Serratrice GT. The diagnosis of amyotrophic lateral sclerosis. *Adv Neurol* 1995;68:143–52.
- [5] Traynor BJ, Codd BM, Corr B, Forde C, Frost E, Hardiman OM. Clinical features of amyotrophic lateral sclerosis according to the El Escorial and Airlie House Diagnostic Criteria. *Arch Neurol* 2000;57:1171–6.
- [6] Lyall RA, Donaldson N, Polkey MI, Leigh PN, Moxham J. Respiratory muscle strength and ventilatory failure in amyotrophic lateral sclerosis. *Brain* 2001;124:2000–13.
- [7] Dalakas MC, Elder GE, Hallett M, Ravits J, Baker M, Papadopoulos N, et al. A long-term follow-up study of patients with post-poliomyelitis neuromuscular symptoms. *N Engl J Med* 1986;314:959–63.
- [8] Dalakas MC, Iliia I. Post-polio syndrome: concepts in clinical diagnosis, pathogenesis, and etiology. *Adv Neurol* 1991;56:495–511.
- [9] Dalakas MC. The post-polio syndrome as an evoked clinical entity definition and clinical description. *Ann NY Acad Sci* 1995;753:68–80.
- [10] Halstead LS. Diagnosing postpolio syndrome: inclusion and exclusion criteria. In: Silver JK, Gawne AC, editors. *Postpolio syndrome*. Philadelphia: Hanley & Belfus; 2004. p. 1–20.
- [11] Mulder DW, Rosenbaum RA, Layton DD. Late progression of poliomyelitis or forme fruste amyotrophic lateral sclerosis? *Mayo Clin Proc* 1972;47:756–61.
- [12] Roos RP, Viola MV, Wöllmann R, Hatch MH, Antel JP. Amyotrophic lateral sclerosis with antecedent poliomyelitis. *Arch Neurol* 1980;37:312–3.
- [13] Shimada A, Lange DJ, Hays AP. Amyotrophic lateral sclerosis in an adult following acute paralytic poliomyelitis in early childhood. *Acta Neuropathol* 1999;97:317–21.
- [14] Norris FH, Denys EH, Sang UK. Polio and ALS. *Neurology* 1990;40:1150.
- [15] Annon C, Daube JR, Windebank AJ, Kurland LT. How frequently does classic amyotrophic lateral sclerosis develop in survivors of poliomyelitis? *Neurology* 1990;40:172–4.
- [16] Moriwaka F, Tashiro K, Okumura H, Yamada T. ALS and poliomyelitis. *Neurology* 1991;41:612.
- [17] Okumura H, Kurland LT, Waring SC. Amyotrophic lateral sclerosis and polio: Is there an association? *Ann NY Acad Sci* 1995;753:245–56.
- [18] Dean E, Ross J, Road JD, Courtenay L, Madill KJ. Pulmonary function in individuals with a history of poliomyelitis. *Chest* 1991;100:118–23.
- [19] Mahgoub A, Cohen R, Rossoff LJ. Weakness, daytime somnolence, cough, and respiratory distress in a 77-year-old man with a history of childhood polio. *Chest* 2001;120:659–61.
- [20] Scelsa SN, Yakubov B, Salzman SH. Dyspnea-fasciculation syndrome: early respiratory failure in ALS with minimal motor signs. *Amyotroph Lateral Scler Other Motor Neuron Disord* 2002;3:239–43.
- [21] Truffert A, Lalive PH, Janssens JP, Sinnreich M, Magistris MR. Endplate dysfunction causing respiratory failure in a patient with prior paralytic poliomyelitis. *J Neurol Neurosurg Psychiatry* 2003;74:370–2.
- [22] Ito H, Hirano A. Comparative study of spinal cord ubiquitin expression in post-poliomyelitis and sporadic amyotrophic lateral sclerosis. *Acta Neuropathol* 1994;87:425–9.
- [23] Pezeshkpour GH, Dalakas MC. Long-term changes in the spinal cords of patients with old poliomyelitis: signs of continuous disease activity. *Arch Neurol* 1988;45:505–8.
- [24] Miller DC. Post-polio syndrome spinal cord pathology: case report with immunopathology. *Ann NY Acad Sci* 1995;753:186–93.
- [25] Terao S, Sobue G, Hashizume Y, Mitsuma T, Takahashi A. Disease specific patterns of neuronal loss in the spinal ventral horn in amyotrophic lateral sclerosis, multiple system atrophy and X-linked recessive bulbospinal neuronopathy; with special reference to the loss of small-sized neuron in the intermediate zone. *J Neurol* 1994;241:196–203.
- [26] Terao S, Li M, Hashizume Y, Osano Y, Mitsuma T, Sobue G. Upper motor neuron lesions in stroke patients do not induce anterograde transneuronal degeneration in spinal anterior horn cells. *Stroke* 1997;28:2553–6.
- [27] Terao S, Sobue G, Li M, Hashizume Y, Tanaka F, Mitsuma T. The lateral corticospinal tract and spinal ventral horn in X-linked recessive spinal and bulbar muscular atrophy: a quantitative study. *Acta Neuropathol* 1997;93:1–6.
- [28] Terao S, Li M, Hashizume Y, Mitsuma T, Sobue G. No transneuronal degeneration between human cortical motor neurons and spinal motor neurons. *J Neurol* 1999;246:61–2.
- [29] Iwata M, Hirano A. “Glial bundles” in the spinal cord late after paralytic anterior poliomyelitis. *Ann Neurol* 1978;4:562–3.

Pharmacological induction of heat-shock proteins alleviates polyglutamine-mediated motor neuron disease

Masahisa Katsuno, Chen Sang, Hiroaki Adachi, Makoto Minamiyama, Masahiro Waza, Fumiaki Tanaka, Manabu Doyu, and Gen Sobue*

Department of Neurology, Nagoya University Graduate School of Medicine, 65 Tsurumai-cho, Showa-ku, Nagoya 466-8550, Japan

Edited by L. L. Iversen, University of Oxford, Oxford, United Kingdom, and approved September 29, 2005 (received for review July 22, 2005)

Spinal and bulbar muscular atrophy (SBMA) is an adult-onset motor neuron disease caused by the expansion of a trinucleotide CAG repeat encoding the polyglutamine tract in the first exon of the androgen receptor gene (AR). The pathogenic, polyglutamine-expanded AR protein accumulates in the cell nucleus in a ligand-dependent manner and inhibits transcription by interfering with transcriptional factors and coactivators. Heat-shock proteins (HSPs) are stress-induced chaperones that facilitate the refolding and, thus, the degradation of abnormal proteins. Geranylgeranylacetone (GGA), a nontoxic antiulcer drug, has been shown to potentially induce HSP expression in various tissues, including the central nervous system. In a cell model of SBMA, GGA increased the levels of Hsp70, Hsp90, and Hsp105 and inhibited cell death and the accumulation of pathogenic AR. Oral administration of GGA also up-regulated the expression of HSPs in the central nervous system of SBMA-transgenic mice and suppressed nuclear accumulation of the pathogenic AR protein, resulting in amelioration of polyglutamine-dependent neuromuscular phenotypes. These observations suggest that, although a high dose appears to be needed for clinical effects, oral GGA administration is a safe and promising therapeutic candidate for polyglutamine-mediated neurodegenerative diseases, including SBMA.

spinal and bulbar muscular atrophy | geranylgeranylacetone | androgen receptor | heat-shock factor-1

Expansion of a trinucleotide CAG repeat encoding the polyglutamine tract causes inherited neurodegenerative disorders, including spinal and bulbar muscular atrophy (SBMA), Huntington's disease, dentatorubral pallidolusian atrophy, and several forms of spinocerebellar ataxia (1, 2). All these polyglutamine diseases show progressive and refractory neurological symptoms with selective neuronal cell loss within the susceptible regions of the nervous system. SBMA is a lower motor neuron disease exclusively affecting males and characterized by adult-onset proximal muscle atrophy, weakness, fasciculations, and bulbar involvement (3, 4). The molecular basis of this disease is elongation of a polyglutamine tract in the androgen receptor (AR) protein (5), the toxicity of which is considered a major cause of neurodegeneration in SBMA (6, 7). It has been postulated that pathogenesis in SBMA results from testosterone-dependent accumulation of pathogenic, polyglutamine-expanded AR in the cell nucleus (8, 9). This hypothesis is strongly supported by the observation that intranuclear accumulation of disease-causing protein leads to transcriptional dysregulation, a supposed pathway of neurodegeneration in polyglutamine diseases (10, 11).

Accumulated polyglutamine-containing protein is commonly seen as diffuse nuclear staining or as inclusion bodies, the histopathological hallmarks of polyglutamine diseases. Although inclusion bodies appear to represent a cellular defensive response, diffusely accumulated polyglutamine-containing protein in the nucleus possesses a distinctly toxic property (12–14). Accumulation of pathogenic protein is, thus, a major target of therapeutic

strategies for polyglutamine diseases. This view is supported by animal studies showing that hormonal interventions lowering serum testosterone levels successfully prevents nuclear accumulation of pathogenic AR and, thereby, rescue the phenotypes of mouse models of SBMA (8, 15, 16).

Heat-shock proteins (HSPs) are stress-induced molecular chaperones that play a crucial role in maintaining correct folding, assembly, and intracellular transport of proteins (17, 18). Under toxic conditions, HSP synthesis is rapidly up-regulated and nonnative proteins are refolded. There is increasing evidence that HSPs abrogate polyglutamine toxicity by refolding and solubilizing pathogenic proteins (19–21). Overexpression of Hsp70, together with Hsp40, inhibits toxic accumulation of abnormal polyglutamine protein and suppresses cell death in a variety of cellular models of polyglutamine diseases including SBMA (22–24). Hsp70 has also been shown to facilitate proteasomal degradation of abnormal AR protein in a cell culture model of SBMA (25). The salutary effects of Hsp70 have been verified in studies by using mouse models of polyglutamine diseases (26, 27). However, clinical applications based on these studies have certain limitations because they used genetic overexpression of Hsp70.

Geranylgeranylacetone (GGA) is an acyclic isoprenoid compound with a retinoid skeleton that induces HSP synthesis in various tissues including the gastric mucosa, intestine, liver, myocardium, retina, and central nervous system (28–32). Oral administration of GGA rapidly up-regulates HSP expression in response to a variety of stresses, although this effect is weak under nonstress conditions (29). With an extremely low toxicity, this compound has been widely used as an oral antiulcer drug. The aim of the present study is to investigate whether oral GGA induces HSP expression and thereby suppresses polyglutamine toxicity in cell culture and mouse models of SBMA.

Materials and Methods

Adenovirus Vector. Adenovirus vectors were constructed with the BD Adeno-X Expression system according to the manufacturer's protocol (Invitrogen). Briefly, truncated AR constructs containing GFP (24 CAG repeats, 215 N-terminal amino acids of AR) or 97 CAG repeats, and 442 N-terminal amino acids of AR) (23) were cloned into the pShuttle vector between the NheI and XbaI sites. pShuttle vectors with truncated AR24 or AR97 were digested with I-CeuI and P1-SceI. After *in vitro* ligation, recombinant adenovirus vector constructs containing the respective transgenic fragments were used to transfect HEK293 cells, and the vectors were isolated

Conflict of interest statement: No conflicts declared.

This paper was submitted directly (Track II) to the PNAS office.

Freely available online through the PNAS open access option.

Abbreviations: SBMA, spinal and bulbar muscular atrophy; AR, androgen receptor; GGA, geranylgeranylacetone; HSP, heat-shock protein; HSF-1, heat-shock factor-1.

*To whom correspondence should be addressed. E-mail: sobueg@med.nagoya-u.ac.jp.

© 2005 by The National Academy of Sciences of the USA

by using the freeze–thaw method. Finally, virus titer was determined by using the BD Adeno-X Rapid Titer kit (Invitrogen).

Cell Culture. The human neuroblastoma cell line (SH-SY5Y, American Type Culture Collection No. CRL-2266) was maintained with DMEM/F12 (Invitrogen) supplemented with 10% FCS. After neural differentiation in differentiation medium (DMEM/F12 supplemented with 5% FCS and 10 μ M retinoic acid) for 4 days, SH-SY5Y cells were infected with the recombinant adenovirus vectors containing truncated AR24 or AR97 at a multiplicity of infection of 20 for 1 h and then treated with GGA. At each time point (0, 2, 4, and 6 days) after infection, cells were fixed with 4% paraformaldehyde for 10 min at room temperature, counterstained with propidium iodide (Molecular Probes), and mounted in Gelvatol. A confocal laser scanning microscope (MRC1024, Bio-Rad) and a conventional fluorescent microscope were used to determine the degree of neuronal cell death and the presence of GFP-labeled AR24 or AR97 protein in diffuse nuclear aggregates or in inclusion bodies. Quantitative analyses were made from triplicate determinations. Duplicate slides were graded blindly in two independent trials as described in ref. 23.

Immunocytochemistry. Cells were fixed with 4% paraformaldehyde and incubated with an anti-HSF-1 (HSF-1, heat-shock factor-1) antibody (1:5,000, Stressgen, Victoria, Canada) and anti-rabbit Alexa Fluor 568 antibody (1:1,000, Molecular Probes), then counterstained with Hoechst 33342 (Molecular Probes).

Animals. AR-24Q and AR-97Q mice were generated by using the pCAGGS vector as described in 8 and 33. The mouse rotarod task was performed with an Economex rotarod (Columbus Instruments, Columbus, OH), and cage activity was measured with the AB system (Neuroscience, Tokyo) as described in ref. 34. Each cage contained three mice, which were subjected to a 12-h light/dark cycle. All animal experiments were approved by the Animal Care Committee of Nagoya University Graduate School of Medicine.

GGA Treatment. GGA was a gift from Eisai, Inc. (Tokyo). For treating cultured SH-SY5Y cells, GGA was dissolved in absolute ethanol supplemented with 0.2% α -tocopherol, and ethanol with α -tocopherol alone was used as vehicle. For oral administration to mice, GGA granules were mixed with powdered rodent chow at concentrations of 0.25%, 0.5%, 1%, and 2%. GGA was administered to mice from 6 weeks of age until the end of the analysis without withdrawal or dose reduction. All mice had unlimited access to food and water. Net consumption of GGA was determined based on the amount of food consumed in each cage.

Western Blotting. SH-SY5Y cells were lysed in CellLytic lysis buffer (Sigma–Aldrich) containing a protease inhibitor mixture (Roche Diagnostics). Mouse tissues were homogenized in buffer containing 50 mM Tris (pH 8.0), 150 mM NaCl, 1% Nonidet P-40, 0.5% deoxycholate, 0.1% SDS, and 1 mM 2-mercaptoethanol with 1 mM PMSF, and 6 μ g/ml aprotinin and then centrifuged at $2,500 \times g$ for 15 min. To extract the nuclear and cytoplasmic fractions, mouse tissues were treated with NE-PER nuclear and cytoplasmic extraction reagents (Pierce); cultured cells were lysed in buffer containing 10 mM TrisHCl (pH 7.4), 10 mM NaCl, 3 mM MgCl₂, and 0.5% Nonidet P-40 and then suspended in buffer containing 50 mM TrisHCl (pH 6.8), 2% SDS, 6% glycerol, and protease inhibitor mixture (Roche Diagnostics). Equal amounts of protein were separated by 5–20% SDS/PAGE and transferred to Hybond-P membranes (Amersham Pharmacia Biotech). Primary antibodies and concentrations were as follows: AR (H-280, 1:1,000, Santa Cruz Biotechnology) Hsp70 (1:1,000, Stressgen Biotechnologies, Victoria, Canada), Hsc70 (1:5,000, Stressgen Biotechnologies), Hsp25 (1:5,000, Stressgen Biotechnologies), Hsp40 (1:5,000, Stressgen Biotechnologies), Hsp60 (1:5,000, Stressgen Biotechnologies),

Grp78 (1:5,000, Stressgen Biotechnologies), Hsp90 (1:1,000, Stressgen Biotechnologies), Hsp105 (1:250, Novocastra Laboratories, Newcastle, U.K.), HSF-1 (1:5,000, Stressgen Biotechnologies), and thioredoxin (1:2,000, Redox Bioscience, Kyoto, Japan). Primary antibody binding was probed with horseradish peroxidase-conjugated secondary antibodies at a dilution of 1:5,000, and bands were detected by using immunoreaction enhance solution (Can Get Signal, Toyobo, Japan) and enhanced chemiluminescence (ECL Plus, Amersham Biosciences, which is now GE Healthcare). An LAS-3000 imaging system (Fuji) was used to produce digital images. Signal intensities of three independent blots were quantified with IMAGE GAUGE software version 4.22 (Fuji) and expressed in arbitrary units. Membranes were reprobed with anti- α -tubulin (1:5,000, Santa Cruz Biotechnology), or anti-histone H3 (1:500, Upstate Biotechnology, Lake Placid, NY) antibodies for normalization.

Immunohistochemistry. Mice anesthetized with ketamine-xylazine were perfused with 4% paraformaldehyde fixative in phosphate buffer (pH 7.4). Tissues were dissected, postfixed in 10% phosphate-buffered formalin, and processed for paraffin embedding. Sections to be stained with anti-polyglutamine antibody 1C2 were treated with formic acid for 5 min at room temperature; those to be incubated with anti-HSF-1 antibody were boiled in 10 mM citrate buffer for 15 min. Primary antibodies and dilutions were as follows: polyglutamine (1:20,000, Chemicon, Temecula, CA), Hsp70 (1:500, Stressgen Biotechnologies), and anti-HSF-1 (1:5,000, Stressgen Biotechnologies). Primary antibody binding was probed with a labeled polymer of secondary antibody as part of the Envision+ system containing horseradish peroxidase (DakoCytomation, Gostrup, Denmark). The number of 1C2-positive cells in the spinal cord and muscle were determined as described in ref. 27.

Statistical Analyses. We analyzed data by using the Kaplan–Meier and log-rank test for survival rate, ANOVA with Dunnett's post hoc test for multiple comparisons, and an unpaired t test from STATVIEW software version 5 (Hulinks, Tokyo).

Results

GGA Suppresses Polyglutamine Toxicity in Cellular Model of SBMA. To test whether GGA suppresses cellular toxicity induced by expanded polyglutamine, we generated a cultured cell model of SBMA. Adenovirus vector-mediated expression of a truncated AR with 97 CAGs (tAR97Q) resulted in the formation of inclusion bodies in the nucleus and cytoplasm as well as eventual cell death in human neuroblastoma cell line SH-SY5Y, whereas expression of AR containing only 24 CAGs (tAR24Q) showed no such toxicity (Fig. 1 A and B). GGA administration reduced neuronal cell death as detected by propidium iodide staining in the cells expressing tAR97Q, the strongest effect occurring at a dose of 10^{-9} M (Fig. 1 B and C). Although GGA failed to decrease the number of the cells containing inclusion bodies, Western blot analysis using an anti-AR N terminus antibody demonstrated that GGA significantly diminished the amount of a high-molecular-weight complex, which likely corresponds to oligomers of tAR97Q (Fig. 1 D and E) (35). Thus, GGA treatment suppresses cytotoxicity caused by accumulation of AR with elongated polyglutamine without inhibiting inclusion body formation.

GGA Induces HSPs in Cellular Model of SBMA. To determine whether the GGA-mediated mitigation of polyglutamine toxicity is due to HSP expression, we determined HSP levels in the cell culture model of SBMA after GGA treatment. GGA up-regulated expression of Hsp70, Hsp90, and Hsp105 in the cells with tAR97Q but did not in those with tAR24Q (Fig. 2 A and B). Cycloheximide treatment eliminated GGA-mediated HSP induction and suppression of cell death (Fig. 2 C and D). Expression of Hsc70, a constitutively expressed HSP, was not increased by GGA treatment; no GGA-mediated up-regulation was detected for other HSPs tested, such as

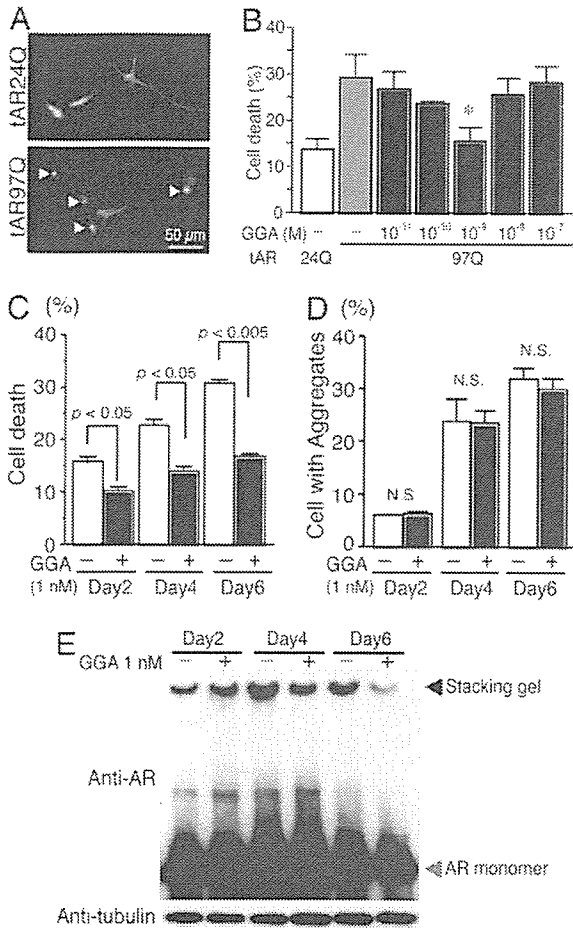


Fig. 1. Effects of GGA on polyglutamine toxicity in cultured cell. (A) Punctuated aggregates visualized with GFP (arrowhead) are formed in SHSY-5Y cells infected with an adenovirus vector containing truncated AR with 97 CAGs (tAR97Q-GFP) but not in those bearing tAR24Q. (B) Frequency of cell death 6 days after infection as detected by propidium iodine staining (*, $P < 0.05$ compared with untreated tAR97Q cells). (C) Suppression of cell death by GGA. (D) Frequency of cells bearing aggregates. (E) Anti-AR analysis of Western blots of extracts from cells infected with tAR97Q. Error bars indicate SD.

Hsp40 and Hsp60, or for thioredoxin, a redox-regulating protein (data not shown). Western blotting (Fig. 2 E and F) and immunocytochemistry (Fig. 2G) revealed that GGA increased the nuclear uptake of hyperphosphorylated HSF-1, a transcription factor regulating HSP expression in the nucleus. Given that activated HSF-1 forms a hyperphosphorylated trimer and translocates into the nucleus, these findings suggest that GGA activates HSF-1, leading to HSP up-regulation.

GGA Ameliorates Symptomatic Phenotypes of SBMA Mouse. To examine whether pharmacological induction of HSPs alleviates polyglutamine-dependent neuronal dysfunction, oral GGA was administered to transgenic mice bearing human AR with 97 CAGs (AR-97Q). The actual amount of GGA was constant in each treatment group during the treatment period (see Table 1, which is published as supporting information on the PNAS web site). Oral GGA ameliorated muscle atrophy, gait disturbance, rotarod disability, and body weight loss in AR-97Q mice at both doses of 0.5 and 1% of food, which correspond to ≈ 600 and $1,200 \text{ mg kg}^{-1} \text{ day}^{-1}$, respectively (Fig. 3 A–E and Table 1). The life span of AR-97Q mice treated orally with 0.5 or 1% GGA was significantly extended compared with that of untreated AR-97Q mice. ($P < 0.001$) (Fig. 3F). GGA failed to alleviate motor dysfunction in

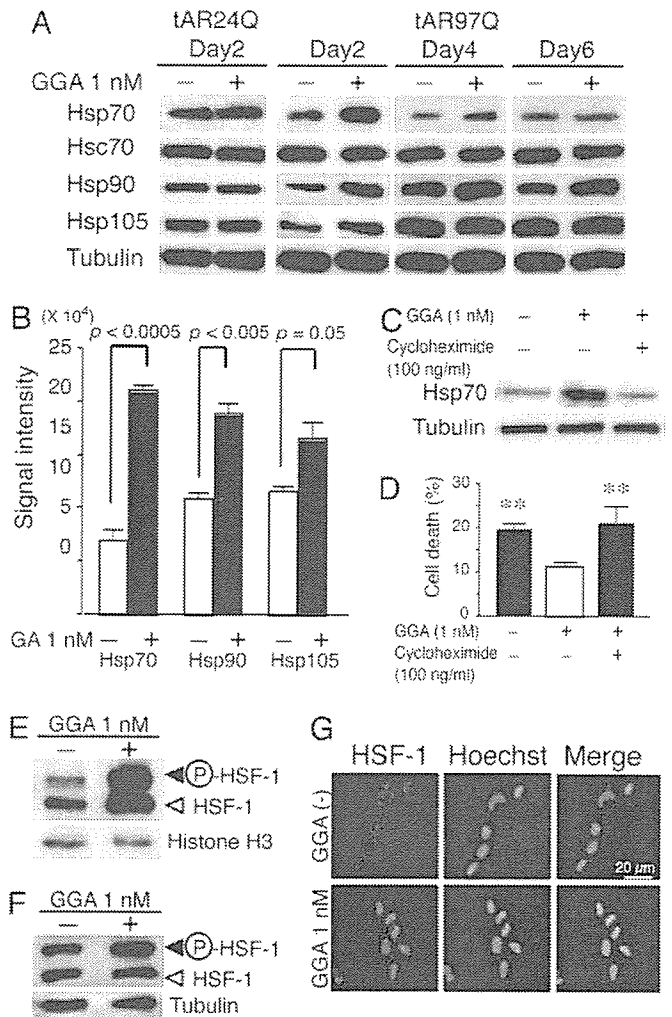


Fig. 2. GGA-mediated HSP induction in cultured cell. (A) Anti-HSP analysis of Western blots from cells infected with tAR97Q and treated with GGA. (B) Quantification of the levels of HSPs from tAR97Q-infected cells after 2 days of GGA treatment. (C) Anti-Hsp70 analysis of Western blots from tAR97Q cells treated with or without cycloheximide. (D) Frequency of cell death 2 days after infection as detected by propidium iodine staining (**, $P < 0.05$ compared with tAR97Q cells treated with GGA but not with cycloheximide). (E and F) Anti-HSF-1 analysis of Western blots of the cellular nuclear fraction (E) and that of total cell lysate (F). Upper bands correspond to the hyperphosphorylated, active form of HSF-1. (G) Immunocytochemistry for HSF-1. Error bars indicate SD.

AR-97Q mice at a dose of 0.25%. A higher dose of GGA, 2% of food, inhibited body growth and had no beneficial effects on the neurological phenotypes of the AR-97Q mice. Although no hepatic or renal toxicity was demonstrated at other doses, this high dose caused liver enlargement and dysfunction in wild-type and transgenic mice (see Table 2, which is published as supporting information on the PNAS web site).

GGA Induces HSP Expression in SBMA Mice Through HSF-1 Activation. To examine whether the GGA-induced improvement in the phenotypes of AR-97Q mice was due to induction of HSPs, the expression levels of HSPs were determined. Oral GGA increased the expression of Hsp70, Hsp90, and Hsp105 in the central nervous system and in the skeletal muscle of AR-97Q mice at the doses (0.5 and 1% of food) that were shown to improve symptomatic phenotypes of AR-97Q mice (Fig. 4 A–C and Fig. 6 A and B, which is published as supporting information on the PNAS web site). The

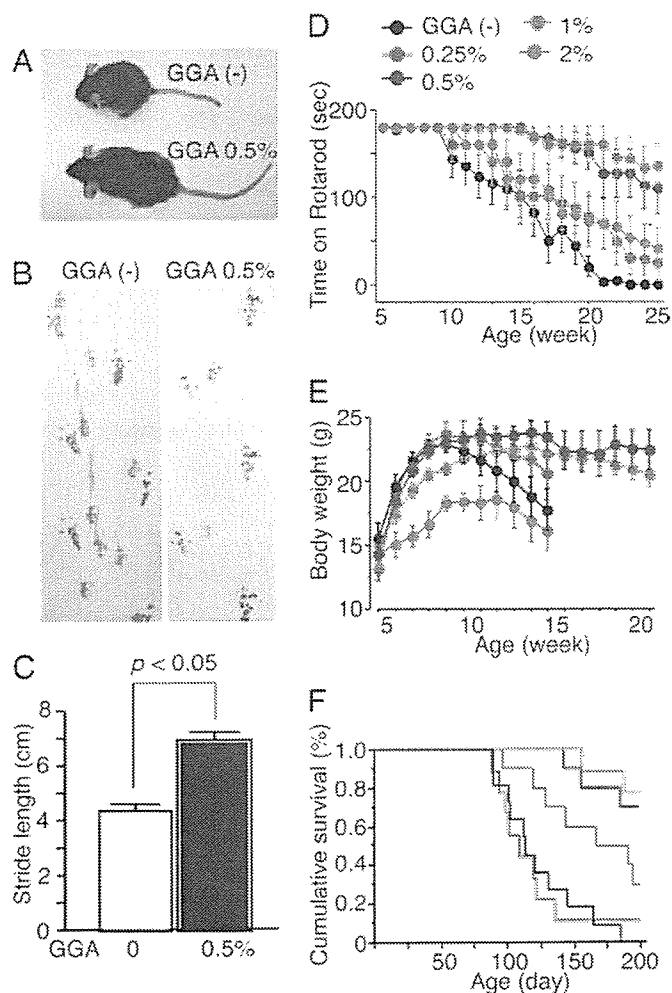


Fig. 3. Effect of GGA on neurological phenotypes of AR-97Q mice. (A) Muscle atrophy of 13-week AR-97Q mice. (B) Footprints of 13-week AR-97Q mice. Front paws are shown in red, and hind paws are shown in blue. (C) Stride distance of 13-week AR-97Q mice ($n = 3$ for each group). (D-F) Rotarod task (D), body weight (E), and cumulative survival (F) of male AR-97Q mice treated with GGA ($n = 12$ for each group) and untreated counterparts ($n = 15$). Rotarod performance significantly improved after GGA at doses of 0.5% and 1.0% ($P < 0.0001$ at both doses compared with nontreated mice at 20 weeks), and body weight increased significantly at a dose of 0.5% ($P < 0.005$ at 0.5% and $P < 0.05$ at 1.0%, at 14 weeks). Error bars indicate SD.

induction of HSPs was not clearly observed in the central nervous system until 3 weeks after treatment initiation, but it continued for at least 4 weeks thereafter (see Fig. 7A, which is published as supporting information on the PNAS web site). HSP induction by GGA was undetectable at a dose of 0.25% and was not significant at 2%, in agreement with the lack of therapeutic effect on motor function at these doses. Grp78, Hsp25, Hsp40, Hsp60, and thioredoxin were not induced by GGA administration (see Fig. 7B).

To examine whether GGA induced HSP expression through HSF-1 activation, the nuclear translocation of HSF-1 was investigated after GGA treatment. In the untreated state, the level of nuclear accumulated hyperphosphorylated HSF-1 in the central nervous systems of AR-97Q mice was lower than in the wild-type mice. However, when AR-97Q mice received 0.5% oral GGA, nuclear translocation of HSF-1 was higher than in the nontreated mice (Fig. 4D and Fig. 8, which is published as supporting information on the PNAS web site). In contrast, nuclear translocation of HSF-1 in skeletal muscle of untreated AR-97Q mice is already

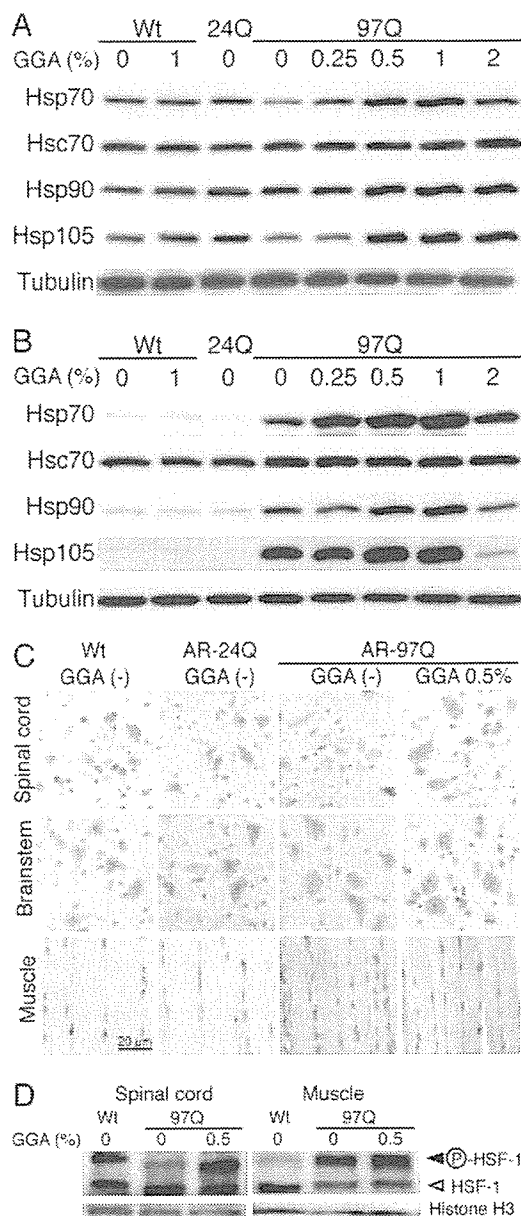


Fig. 4. GGA-mediated HSP induction in AR-97Q mice. (A) Western blotting for various HSPs in the spinal cord of 14-week, wild-type (Wt), AR-24Q and AR-97Q mice. (B) Western blotting for various HSPs in skeletal muscle of 14-week wild-type, AR-24Q, and AR-97Q mice. (C) Immunohistochemistry for Hsp70 in 14-week wild-type, AR-24Q, and AR-97Q mice. (D) Western blotting of nuclear fraction from spinal cord and that from muscle using anti-HSF-1 antibody. Upper bands correspond to the hyperphosphorylated active form of HSF-1.

much higher than in wild-type mice, thus perhaps explaining the high degree of Hsp70 induction in AR-97Q mice. After GGA treatment, nuclear translocation of HSF-1 in skeletal muscle of AR-97Q mice was even higher than it was in untreated AR-97Q mice, contributing to a higher induction of Hsp70 (Figs. 4D and 8). These experiments suggest that oral GGA restores activation of HSF-1, which is inhibited by expanded polyglutamine in the affected nervous tissues of AR-97Q mice.

GGA Inhibits Accumulation of Pathogenic AR in Nucleus. With the aim of evaluating the effect of GGA on the nuclear accumulation of abnormal AR, immunohistochemistry with anti-polyglutamine an-

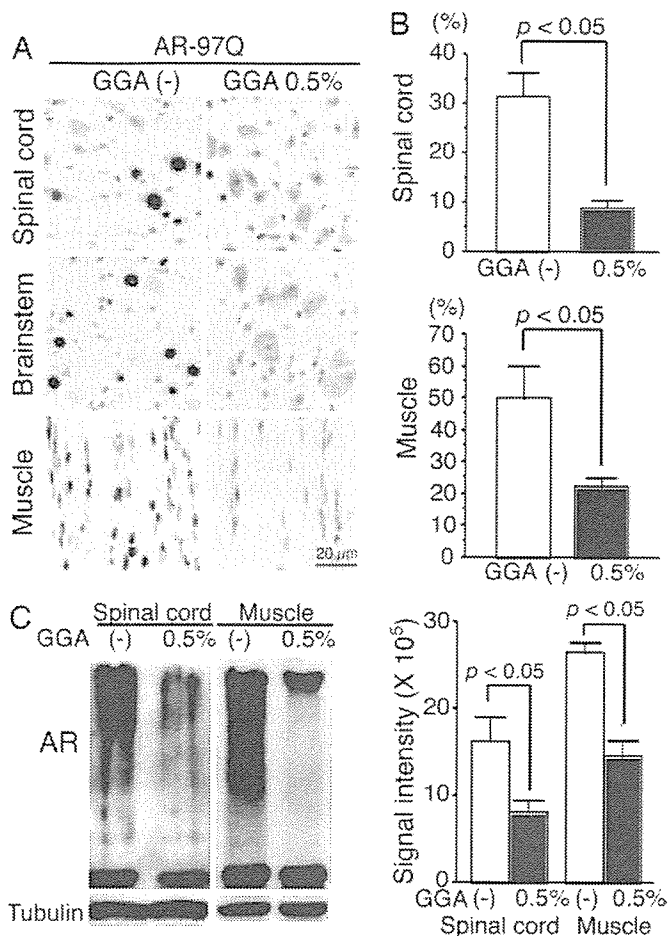


Fig. 5. Effect of GGA on accumulation of abnormal AR. (A) Immunohistochemistry of 14-week wild-type, AR-24Q, and AR-97Q mice using 1C2 antibody. (B) Quantification of 1C2-positive cells in spinal cord and muscle of AR-97Q mice treated with or without GGA. (C) Western blotting for AR of 14-week AR-97Q mice and quantification of the high-molecular-weight, abnormal AR complex indicated by a smear from the top of the gel. Error bars indicate SD.

tibody 1C2 was performed on tissues from GGA-administrated and untreated AR-97Q mice. Oral 0.5% GGA decreased the number of 1C2-positive cells in nervous tissues and, to a lesser extent, in muscle (Fig. 5 A and B). Western blot analysis using an antibody against AR demonstrated that 0.5% oral GGA reduced the amount of the high-molecular-weight complex of abnormal AR (Fig. 5C). These findings suggest that oral GGA-mediated HSP induction inhibits nuclear accumulation of abnormal AR, leading to mitigation of polyglutamine-dependent pathogenesis.

Discussion

GGA Induces HSP Expression. In the present study, GGA induced Hsp70, Hsp90, and Hsp105 in a cultured cell model of SBMA, leading to abrogation of polyglutamine-mediated cytotoxicity. Furthermore, oral GGA alleviated neuronal dysfunction through induction of HSPs in SBMA mice.

GGA was first introduced as a nontoxic inducer of Hsp70 in rat gastric mucosa (28). Oral GGA has also been reported to induce Hsp70 in the central nervous system as well as in the small intestine, liver, heart, and retina of rodents without any adverse effects (29–32, 36, 37). The present study suggests that the required dose for HSP induction in the SBMA mouse model is $\approx 600 \text{ mg kg}^{-1} \text{ day}^{-1}$, whereas $200 \text{ mg kg}^{-1} \text{ day}^{-1}$ induces HSP expression in nonneuronal tissues of rodents under stress (28, 36). Several

studies have verified that Hsp70 induction is due to GGA-mediated activation of HSF-1, a transcription factor that regulates expression of Hsp70 (28, 37). In the SBMA mice, GGA facilitated nuclear translocation of HSF-1, leading to induction of Hsp70, in the affected tissues.

GGA showed no adverse effects at the salutary doses used in the present study, although hepatic toxicity was detected at a higher dose. Low toxicity of GGA is advantageous, because continuous administration of GGA at a high dose is required for treating slowly progressive neurodegenerative disease (6, 7). Pharmacological induction of HSP by using GGA thus appears to be an applicable therapeutic strategy for SBMA, although careful attention should be paid to adverse effects during long-term treatment.

HSPs as Therapeutics for Polyglutamine Diseases. In the present study, GGA-mediated HSP induction resulted in inhibiting the accumulation of abnormal AR in the cellular and transgenic mouse models of SBMA. Accumulation of abnormal protein has been considered central to the pathogenesis of polyglutamine diseases, including SBMA. It has been postulated that expanded polyglutamine confers a monomeric protein conformational change from random coil to β -sheet, leading to formation of a polyglutamine oligomer (38, 39). The misfolded monomer and oligomer exercise their toxic effects by interacting with normal cellular proteins. Direct inhibition of polyglutamine oligomerization by Congo red has been demonstrated to exert therapeutic effects in a mouse model of Huntington's disease (40). Whereas oligomerization of causative proteins has been implicated in the pathogenic processes of neurodegeneration in polyglutamine diseases, the formation of inclusion bodies or mature amyloid fibrils appears to possess cytoprotective properties (13, 41). Based on this hypothesis, HSPs have been drawing a great deal of attention because they inhibit oligomer assembly and thereby mitigate polyglutamine toxicity (20, 21, 38). This view is supported by the fact that overexpression of Hsp70 attenuates the accumulation of polyglutamine-containing protein, resulting in amelioration of neurodegeneration in animal models of spinocerebellar ataxias or SBMA (26, 27).

GGA treatment significantly suppressed nuclear accumulation of abnormal AR in SBMA mice but did not inhibit inclusion body formation in cultured cells. This inconsistency does not necessarily deny a beneficial effect of GGA on polyglutamine aggregation, because it can be explained by several lines of evidence: (i) HSPs facilitate amyloid fibril formation by stabilizing the conformation of abnormal polyglutamine-expanded protein (42), and (ii) HSPs biochemically alter the structure of inclusion bodies (43, 44).

Hsp70 overexpression, however, fails to alleviate neurodegeneration or aggregate formation in the R6/2 mouse model of Huntington's disease (45, 46). This discord appears to indicate that higher levels of Hsp70 or the concomitant induction of other HSPs is required to alleviate Huntington's disease pathology. In addition to Hsp70, various molecular chaperones that colocalize with aggregates have also been shown to suppress polyglutamine toxicity: Hsp40-associated Hsp70 (23, 43), Hsp90, and Hsp105 (47, 48). Oral GGA induced Hsp90 and Hsp105 in the mouse model of SBMA and such diverse HSP up-regulation might contribute to the beneficial effects of GGA in the SBMA mice.

HSP in Pathogenesis of polyQ Diseases. Not only are HSPs considered potent suppressors of polyglutamine toxicity, but they are also implicated in the pathogenesis of neurodegeneration (20). There are several lines of evidence that polyglutamine elongation weakens the protective responses for coping with cellular stress. Truncated AR with expanded polyglutamine delays the induction of Hsp70 after heat shock (49). In the SBMA mice we examined, the level of Hsp70 in spinal cord was decreased before the onset of motor dysfunction. A similar finding has also been reported in the R6/2 mouse model of Huntington's disease (46).

In our SBMA mice, abnormal, polyglutamine-expanded AR seems to inhibit nuclear translocation of HSF-1 in the central nervous system, leading to a decrease in the level of Hsp70. In mammalian cells, induction of Hsp70 requires activation and nuclear localization of HSF-1. In the presence of nonnative protein, HSF-1 is derepressed, forming a trimer that translocates into the nucleus and binds to heat-shock elements within the gene encoding Hsp70 (50). In cellular models, this stress-induced nuclear accumulation of HSF-1 has been designated nuclear granules (51). Aggregates of abnormal ataxin-1, the causative protein in spinocerebellar ataxia 1, have been shown to hinder induction of nuclear granules in response to heat shock (52). Therefore, failure of HSF-1 activation appears to enhance polyglutamine toxicity. In this context, it is intriguing that inhibition of the nuclear accumulation of HSF-1 was detected in spinal cord but not in muscle of SBMA transgenic mice. Given that the threshold for HSP induction is relatively high in motor neurons (53), motor-neuron-specific inactivation of HSP transcription might partially explain why the central nervous system

is selectively affected in polyglutamine diseases including SBMA.

HSP-Based Therapy for Neurodegeneration. Both genetic and pharmacological manipulations of HSPs have been demonstrated to mitigate the pathogenesis of neurodegeneration (54–57). These observations suggest that GGA-mediated HSP induction may provide a therapeutic strategy for diverse neurodegenerative disorders, because these diseases share common pathogenic mechanisms such as abnormal protein aggregation, disruption of the ubiquitin-proteasome system and activation of the apoptotic pathway.

In summary, our observations indicate that GGA is a safe and promising therapeutic approach for treating many devastating neurodegenerative diseases, including SBMA.

We thank Eisai, Inc. for providing GGA. This work was supported by a Center-of-Excellence grant from the Ministry of Education, Culture, Sports, Science and Technology of Japan and grants from the Ministry of Health, Labor, and Welfare of Japan.

- Zoghbi, H. Y. & Orr, H. T. (2000) *Annu. Rev. Neurosci.* 23, 217–247.
- Ross, C. A. (2002) *Neuron* 35, 819–822.
- Kennedy, W. R., Alter, M. & Sung, J. H. (1968) *Neurology* 18, 671–680.
- Sobue, G., Hashizume, Y., Mukai, E., Hirayama, M., Mitsuma, T. & Takahashi, A. (1989) *Brain* 112, 209–232.
- La Spada, A. R., Wilson, E. M., Lubahn, D. B., Harding, A. E. & Fischbeck, K. H. (1991) *Nature* 352, 77–79.
- Fischbeck, K. H., Lieberman, A., Bailey, C. K., Abel, A. & Merry, D. E. (1999) *Philos. Trans. R. Soc. London B* 354, 1075–1078.
- Katsuno, M., Adachi, H., Tanaka, F. & Sobue, G. (2004) *J. Mol. Med.* 82, 298–307.
- Katsuno, M., Adachi, H., Kume, A., Li, M., Nakagomi, Y., Niwa, H., Sang, C., Kobayashi, Y., Doyu, M. & Sobue, G. (2002) *Neuron* 35, 843–854.
- Takeyama, K., Ito, S., Yamamoto, A., Tanimoto, H., Furutani, T., Kanuka, H., Miura, M., Tabata, T. & Kato, S. (2002) *Neuron* 35, 855–864.
- Nucifora, F. C., Jr., Sasaki, M., Peters, M. F., Huang, H., Cooper, J. K., Yamada, M., Takahashi, H., Tsuji, S., Troncoso, J., Dawson, V. L., Dawson, T. M. & Ross, C. A. (2001) *Science* 291, 2423–2428.
- Minamiyama, M., Katsuno, M., Adachi, H., Waza, M., Sang, C., Kobayashi, Y., Tanaka, F., Doyu, M., Inukai, A. & Sobue, G. (2004) *Hum. Mol. Genet.* 13, 1183–1192.
- Yamada, M., Wood, J. D., Shimohata, T., Hayashi, S., Tsuji, S., Ross, C. A. & Takahashi, H. (2001) *Ann. Neurol.* 49, 14–23.
- Arrasate, M., Mitra, S., Schweitzer, E. S., Segal, M. R. & Finkbeiner, S. (2004) *Nature* 431, 805–810.
- Adachi, H., Katsuno, M., Minamiyama, M., Waza, M., Sang, C., Nakagomi, Y., Kobayashi, Y., Tanaka, F., Doyu, M. & Inukai, A., et al. (2005) *Brain* 128, 659–670.
- Katsuno, M., Adachi, H., Doyu, M., Minamiyama, M., Sang, C., Kobayashi, Y., Inukai, A. & Sobue, G. (2003) *Nat. Med.* 9, 768–773.
- Chevalier-Larsen, E. S., O'Brien, C. J., Wang, H., Jenkins, S. C., Holder, L., Lieberman, A. P. & Merry, D. E. (2004) *J. Neurosci.* 24, 4778–4786.
- Welch, W. J. & Brown, C. R. (1996) *Cell Stress Chaperones* 1, 109–115.
- Morimoto, R. I. & Santoro, M. G. (1998) *Nat. Biotechnol.* 16, 833–838.
- Kobayashi, Y. & Sobue, G. (2001) *Brain Res. Bull.* 56, 165–168.
- Wytenbach, A. (2004) *J. Mol. Neurosci.* 23, 69–96.
- Muchowski, P. J. & Wacker, J. L. (2005) *Nat. Rev. Neurosci.* 6, 11–22.
- Cummings, C. J., Mancini, M. A., Antalffy, B., DeFranco, D. B., Orr, H. T. & Zoghbi, H. Y. (1998) *Nat. Genet.* 19, 148–154.
- Kobayashi, Y., Kume, A., Li, M., Doyu, M., Hata, M., Ohtsuka, K. & Sobue, G. (2000) *J. Biol. Chem.* 275, 8772–8778.
- Wytenbach, A., Swartz, J., Kita, H., Thykjaer, T., Carmichael, J., Bradley, J., Brown, R., Maxwell, M., Schapira, A., Orntoft, T. F., et al. (2001) *Hum. Mol. Genet.* 10, 1829–1845.
- Bailey, C. K., Andriola, I. F., Kampinga, H. H. & Merry, D. E. (2002) *Hum. Mol. Genet.* 11, 515–523.
- Cummings, C. J., Sun, Y., Opal, P., Antalffy, B., Mestril, R., Orr, H. T., Dillmann, W. H. & Zoghbi, H. Y. (2001) *Hum. Mol. Genet.* 10, 1511–1518.
- Adachi, H., Katsuno, M., Minamiyama, M., Sang, C., Pagoulatos, G., Angelidis, C., Kusakabe, M., Yoshiki, A., Kobayashi, Y., Doyu, M. & Sobue, G. (2003) *J. Neurosci.* 23, 2203–2211.
- Hirakawa, T., Rokutan, K., Nikawa, T. & Kishi, K. (1996) *Gastroenterology* 111, 345–357.
- Yamagami, K., Yamamoto, Y., Ishikawa, Y., Yonezawa, K., Toyokuni, S. & Yamaoka, Y. (2000) *J. Lab. Clin. Med.* 135, 465–475.
- Ooie, T., Takahashi, N., Saikawa, T., Nawata, T., Arikawa, M., Yamanaka, K., Hara, M., Shimada, T. & Sakata, T. (2001) *Circulation* 104, 1837–1843.
- Ishii, Y., Kwong, J. M. & Caprioli, J. (2003) *Invest. Ophthalmol. Vis. Sci.* 44, 1982–1992.
- Fujiki, M., Kobayashi, H., Abe, T. & Ishii, K. (2003) *Brain Res.* 991, 254–257.
- Niwa, H., Yamamura, K. & Miyazaki, J. (1991) *Gene* 108, 193–199.
- Adachi, H., Kume, A., Li, M., Nakagomi, Y., Niwa, H., Do, J., Sang, C., Kobayashi, Y., Doyu, M. & Sobue, G. (2001) *Hum. Mol. Genet.* 10, 1039–1048.
- Iuchi, S., Hoffner, G., Verbeke, P., Djian, P. & Green, H. (2003) *Proc. Natl. Acad. Sci. USA* 100, 2409–2414.
- Tsuruma, T., Yagihashi, A., Koide, S., Araya, J., Tarumi, K., Watanabe, N. & Hirata, K. (1999) *Transplant Proc.* 31, 572–573.
- Yamanaka, K., Takahashi, N., Ooie, T., Kaneda, K., Yoshimatsu, H. & Saikawa, T. (2003) *J. Mol. Cell Cardiol.* 35, 785–794.
- Sakahira, H., Breuer, P., Hayer-Hartl, M. K. & Hartl, F. U. (2002) *Proc. Natl. Acad. Sci. USA* 99, 16412–16418.
- Perutz, M. F., Pope, B. J., Owen, D., Wanker, E. E. & Scherzinger, E. (2002) *Proc. Natl. Acad. Sci. USA* 99, 5596–5600.
- Sanchez, I., Mahlke, C. & Yuan, J. (2003) *Nature* 421, 373–379.
- Wacker, J. L., Zareie, M. H., Fong, H., Sarikaya, M. & Muchowski, P. J. (2004) *Nat. Struct. Mol. Biol.* 11, 1215–1222.
- Hsu, A. L., Murphy, C. T. & Kenyon, C. (2003) *Science* 300, 1142–1145.
- Muchowski, P. J., Schaffar, G., Sittler, A., Wanker, E. E., Hayer-Hartl, M. K. & Hartl, F. U. (2000) *Proc. Natl. Acad. Sci. USA* 97, 7841–7846.
- Chan, H. Y., Warrick, J. M., Gray-Board, G. L., Paulson, H. L. & Bonini, N. M. (2000) *Hum. Mol. Genet.* 9, 2811–2820.
- Hansson, O., Nylandsted, J., Castilho, R. F., Leist, M., Jaattela, M. & Brundin, P. (2003) *Brain Res.* 970, 47–57.
- Hay, D. G., Sathasivam, K., Tobaben, S., Stahl, B., Marber, M., Mestril, R., Mahal, A., Smith, D. L., Woodman, B. & Bates, G. P. (2004) *Hum. Mol. Genet.* 13, 1389–1405.
- Mitsui, K., Nakayama, H., Akagi, T., Nekooki, M., Ohtawa, K., Takio, K., Hashikawa, T. & Nukina, N. (2002) *J. Neurosci.* 22, 9267–9277.
- Ishihara, K., Yamagishi, N., Saito, Y., Adachi, H., Kobayashi, Y., Sobue, G., Ohtsuka, K. & Hatayama, T. (2003) *J. Biol. Chem.* 278, 25143–25150.
- Cowan, K. J., Diamond, M. I. & Welch, W. J. (2003) *Hum. Mol. Genet.* 12, 1377–1391.
- Santoro, M. G. (2000) *Biochem. Pharmacol.* 59, 55–63.
- Morimoto, R. I. (1998) *Genes Dev.* 12, 3788–3796.
- Rimoldi, M., Servadio, A. & Zimmarino, V. (2001) *Brain Res. Bull.* 56, 353–362.
- Batulan, Z., Shinder, G. A., Minotti, S., He, B. P., Doroudchi, M. M., Nalbantoglu, J., Strong, M. J. & Durham, H. D. (2003) *J. Neurosci.* 23, 5789–5798.
- Kieran, D., Kalmar, B., Dick, J. R., Riddoch-Contreras, J., Burnstock, G. & Greensmith, L. (2004) *Nat. Med.* 10, 402–405.
- Auluck, P. K., Chan, H. Y., Trojanowski, J. Q., Lee, V. M. & Bonini, N. M. (2002) *Science* 295, 865–868.
- Kikuchi, S., Shingo, K., Takeuchi, M., Tsuji, S., Yabe, I., Niino, M. & Tashiro, K. (2002) *J. Neurosci. Res.* 69, 373–381.
- Waza, M., Adachi, H., Katsuno, M., Minamiyama, M., Sang, C., Tanaka, F., Inukai, A., Doyu, M. & Sobue, G. (2005) *Nat. Med.* 11, 1088–1095.

17-AAG, an Hsp90 inhibitor, ameliorates polyglutamine-mediated motor neuron degeneration

Masahiro Waza^{1,2}, Hiroaki Adachi^{1,2}, Masahisa Katsuno¹, Makoto Minamiyama¹, Chen Sang¹, Fumiaki Tanaka¹, Akira Inukai¹, Manabu Doyu¹ & Gen Sobue¹

Heat-shock protein 90 (Hsp90) functions as part of a multichaperone complex that folds, activates and assembles its client proteins. Androgen receptor (AR), a pathogenic gene product in spinal and bulbar muscular atrophy (SBMA), is one of the Hsp90 client proteins. We examined the therapeutic effects of 17-allylamino-17-demethoxygeldanamycin (17-AAG), a potent Hsp90 inhibitor, and its ability to degrade polyglutamine-expanded mutant AR. Administration of 17-AAG markedly ameliorated motor impairments in the SBMA transgenic mouse model without detectable toxicity, by reducing amounts of monomeric and aggregated mutant AR. The mutant AR showed a higher affinity for Hsp90-p23 and preferentially formed an Hsp90 chaperone complex as compared to wild-type AR; mutant AR was preferentially degraded in the presence of 17-AAG in both cells and transgenic mice as compared to wild-type AR. 17-AAG also mildly induced Hsp70 and Hsp40. 17-AAG would thus provide a new therapeutic approach to SBMA and probably to other related neurodegenerative diseases.

Hsp90, which accounts for 1–2% of cytosolic protein, is one of the most abundant cellular chaperone proteins¹. It functions in a multi-component complex of chaperone proteins including Hsp70, Hop (Hsp70 and Hsp90 organizing protein), Cdc37, Hsp40 and p23. Hsp90 is involved in the folding, activation and assembly of several proteins, known as Hsp90 client proteins¹. As numerous oncoproteins have been shown to be Hsp90 client proteins¹, Hsp90 inhibitors have become a new strategy in antitumor therapy². Geldanamycin, a classical Hsp90 inhibitor, is known as a potent antitumor agent²; however, it has not been used in clinical trials because of its liver toxicity³. 17-AAG is a new derivative of geldanamycin that shares its important biological activities⁴ but shows less toxicity⁵.

Hsp90 requires several interacting co-chaperone proteins to exert its function on Hsp90 client proteins in Hsp90 complexes¹, of which two main forms exist⁶. One complex is a proteasome-targeting form associated with Hsp70 and Hop, and the other is a stabilizing form with Cdc37 and p23 (refs. 7,8). Particularly, p23 is thought to modulate Hsp90 activity in the last stages of the chaperoning pathway, leading to stabilized Hsp90 client proteins⁹. Hsp90 inhibitors, including 17-AAG, inhibit the progression of the Hsp90 complex toward the stabilizing form^{10–12}, and shift it to the proteasome-targeting form^{7,8}, resulting in enhanced proteasomal degradation of the Hsp90 client protein^{7,13–18}.

Because 17-AAG has less toxicity and higher selectivity for client oncoproteins¹⁹, 17-AAG is now in clinical trials for a wide range of malignancies²⁰. Additionally, Hsp90 inhibitors also function as Hsp inducers^{20,21}. Several previous studies have suggested that Hsp90 inhibitors could be applied to nononcological diseases as neuroprotective agents based on their induction of Hsps^{22–28}.

Androgen receptor (AR) is one of the Hsp90 client proteins¹⁵, and is a pathogenic gene product of spinal and bulbar muscular atrophy (SBMA), one of the polyglutamine (polyQ) diseases²⁹. This disease is characterized by premature muscular exhaustion, slow progressive muscular weakness, atrophy and fasciculation in bulbar and limb muscles³⁰. PolyQ diseases are inherited neurodegenerative disorders caused by the expansion of a trinucleotide CAG repeat in the causative genes³¹. In SBMA, the number of polymorphic CAG repeats is normally 14–32, whereas it is expanded to 40–62 CAGs in the AR gene³². A correlation exists between CAG repeat size and disease severity³³. The pathologic features of SBMA are motor neuron loss in the spinal cord and brainstem³⁰, and diffuse nuclear accumulation and nuclear inclusions of the mutant AR in the residual motor neurons and certain visceral organs³⁴.

We have already examined several therapeutic approaches in a mouse model of SBMA^{35–38}. As a consequence, we confirmed that castration and leuprorelin, a luteinizing hormone-releasing hormone agonist that reduces testosterone release from the testis, substantially rescued motor dysfunction and nuclear accumulation of mutant AR in male transgenic mice^{35,37}. Although this hormonal therapy was effective, it poses the unavoidable difficulty of severe sexual dysfunction³⁷. In addition, this therapy cannot be applied to other polyQ diseases.

Here, we present a new and potent strategy for SBMA therapy with 17-AAG, an Hsp90 inhibitor. Given that Hsp90 inhibitors have two major activities, preferential client protein degradation and Hsp induction, we hypothesized that 17-AAG would degrade mutant AR more effectively than wild-type AR.

¹Department of Neurology, Nagoya University Graduate School of Medicine, 65 Tsurumai-cho, Showa-ku, Nagoya 466-8550, Japan. ²These authors contributed equally to this work. Correspondence should be addressed to G.S. (sobueg@ned.nagoya-u.ac.jp).

Received 25 February; accepted 10 August; published online 11 September 2005; doi:10.1038/nm1298

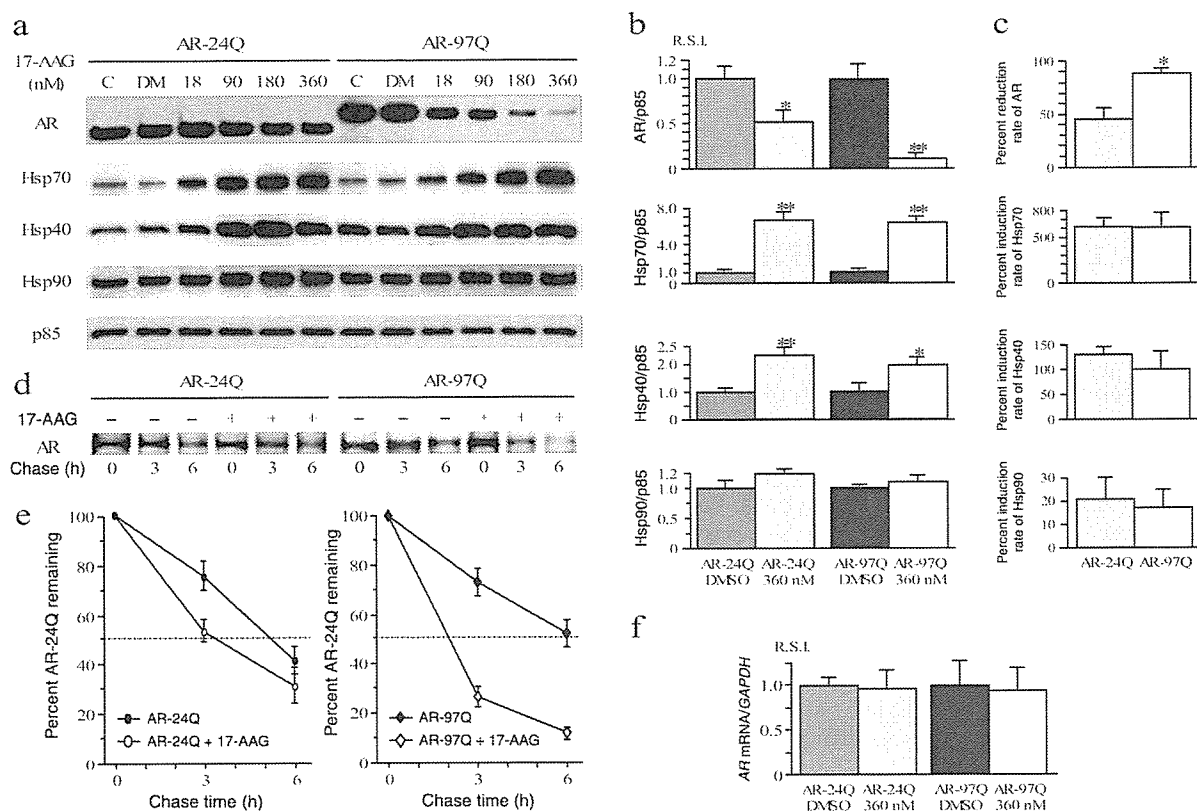


Figure 1 Effect of 17-AAG on the AR or chaperones in cultured-cell models. (a,b) Although the immunoblot and densitometric analysis showed a dose-dependent decline in both wild-type (AR-24Q) and mutant (AR-97Q) AR expression in response to 17-AAG, the mutant AR decreased more than did the wild-type. 17-AAG markedly increased the expression of Hsp70 and Hsp40, especially for Hsp70, but only slightly increased Hsp90 expression. (c) The decrease in mutant AR after treatment with 17-AAG was much higher than that of wild-type AR (88.9% versus 45.9%, $P = 0.0063$). Values are expressed as mean \pm s.e.m. ($n = 5$). (d) Pulse-chase analysis of two forms of AR. Data from one representative experiment for wild-type and mutant AR. (e) Pulse-chase assessment of the half-life of wild-type and mutant AR. The amounts of AR-24Q and AR-97Q remaining in the absence and presence of 17-AAG are indicated. Values are expressed as mean \pm s.e.m. ($n = 4$). (f) Real-time RT-PCR of wild-type and mutant AR mRNA. Quantities are shown as the ratio to GAPDH mRNA. The wild-type and mutant AR mRNA levels were similar under 17-AAG treatments. Values are expressed as mean \pm s.e.m. ($n = 4$). * $P < 0.025$, ** $P < 0.005$.

In this study, we examine the effects of 17-AAG on a cultured-cell model and the transgenic mouse model of SBMA. We show that the mutant AR exists more frequently as a stabilized Hsp90 chaperone complex than does the wild-type AR, and that 17-AAG selectively degrades the mutant AR. Administration of 17-AAG inhibits neuronal nuclear accumulation of the mutant AR and considerably ameliorates motor phenotypes of the SBMA model mouse.

RESULTS

Effect of 17-AAG on expression of AR and Hsps in vitro

To address the question of whether 17-AAG promotes the degradation of polyQ-expanded AR, we treated SH-SY5Y cells highly expressing the wild-type (AR-24Q) or mutant (AR-97Q) AR for 48 h with the indicated doses of 17-AAG or with DMSO as control. Although immunoblot analysis showed a dose-dependent decline in both wild-type and mutant AR expression after treatment with 17-AAG (Fig. 1a), the monomeric mutant AR decreased significantly more than did the wild-type ($P = 0.0063$; Fig. 1b,c), suggesting that the mutant AR is more sensitive to 17-AAG than is the wild-type. The expression of Hsp70 and Hsp40 were also markedly increased after treatment with 17-AAG, but Hsp90 was only slightly increased (Fig. 1a,b). There were no significant differences, however, in the levels

of Hsp70, Hsp40 and Hsp90 induction between the wild-type and mutant AR (Fig. 1c).

To determine whether the decrease in AR resulted from protein degradation or from changes in RNA expression, we assessed the turnover of wild-type and mutant AR with a pulse-chase labeling assay. Without treatment, the wild-type and mutant AR were degraded in a similar manner, as previously reported^{39,40}. In the presence of 17-AAG, however, the wild-type and mutant AR had half-lives of 3.5 h and 2 h, respectively (Fig. 1d,e), whereas levels of mRNA encoding the wild-type and mutant AR were quite similar (Fig. 1f). Cell viability did not differ between wild-type and mutant AR transfected cells (data not shown). These data indicate that 17-AAG preferentially degrades the mutant AR protein without cellular toxicity or alteration of mRNA levels.

To address why 17-AAG preferentially degrades mutant AR, we determined the levels of Hsp90, Hop and p23 associated with wild-type or mutant AR in SH-SY5Y cells without 17-AAG treatment (Fig. 2a). Hop and p23 are two essential components of multi-chaperone Hsp90 complexes¹. Without 17-AAG treatment, coimmunoprecipitation from the cell lysates with antibodies to AR showed that p23 was more highly associated with mutant than with wild-type AR (Fig. 2a,b). The total levels of Hsp90, Hop and p23 were similar in the cells transfected with either wild-type or mutant AR (Fig. 2a).



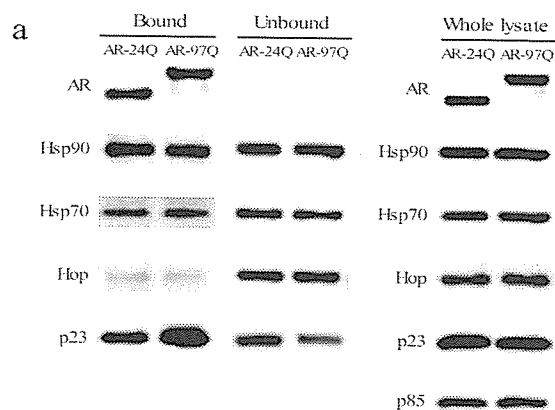


Figure 2 Immunoprecipitation of wild-type and mutant AR in cultured-cell models. (a) Wild-type and mutant AR were immunoprecipitated from cell lysates with an AR-specific antibody and immunoblotted with antibodies to the indicated western blot proteins. There was more mutant AR present in multichaperone complexes with p23 than there was wild-type AR. There were no differences in total expression levels of AR, Hsp90, Hsp70, Hop and p23 between wild-type and mutant AR-expressing cells. Control immunoprecipitations without antibodies did not immunoprecipitate any co-chaperones (data not shown). (b) The densitometric analysis of p23 in the bound and unbound fractions shows there was 1.6 times as much p23 associated with mutant AR than there was with the wild-type ($P < 0.01$). This experiment was repeated with five sets of cells with equivalent results. Values are expressed as mean \pm s.e.m. ($n = 5$). * $P < 0.05$, ** $P < 0.01$. R.S.I., relative signal intensity.

the pharmacological degradation by 17-AAG was dependent on the proteasome system, as previously reported^{17,18}. Furthermore, these results strongly suggest that mutant AR is more likely to be in the Hsp90-p23 multichaperone complexes, which eventually enhances 17-AAG-dependent proteasomal degradation of mutant AR.

Moreover, mutant AR was markedly decreased after treatment with 17-AAG even when induction of Hsp70 and Hsp40 was blocked by the protein-synthesis inhibitor cycloheximide (Supplementary Fig. 1 online), suggesting that 17-AAG contributes to the preferential degradation of mutant AR mainly through Hsp90 chaperone complex formation and subsequent proteasome-dependent degradation rather than through induction of Hsp70 and Hsp40.

17-AAG ameliorates phenotypic expression of SBMA mice
We administered 17-AAG (2.5 or 25 mg/kg) to male transgenic mice carrying full-length human AR-24Q or AR-97Q. The disease progression of AR-97Q mice treated with 25 mg/kg 17-AAG (Tg-25) was

We next examined the status of the Hsp90 chaperone complex in wild-type and mutant AR-expressing cultured cells treated with 17-AAG. Immunoprecipitation with AR-specific antibody showed that Hsp90 chaperone complex-associated Hop was markedly increased, and p23 decreased depending on the dose of 17-AAG (Fig. 3a,b), suggesting that treatment with 17-AAG resulted in the shifting of the AR-Hsp90 chaperone complex from a mature stabilizing form with p23 to a proteasome-targeting form with Hop. The loss of p23 from the mutant AR-Hsp90 complex was significantly higher ($P < 0.005$) than that from the wild-type AR-Hsp90 complex (Fig. 3c). The degradation of wild-type and mutant AR by 17-AAG was completely blocked by the proteasome inhibitor MG132 (Fig. 3d), suggesting that

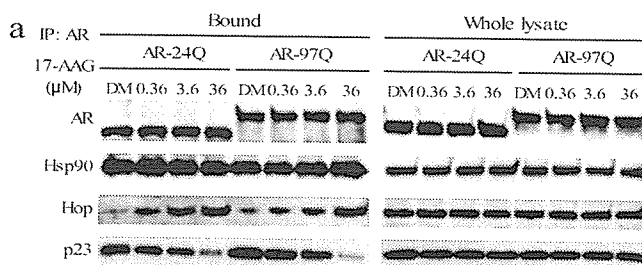


Figure 3 Pharmacological change in the AR-Hsp90 complex, and the correlation to proteasomal degradation. (a) Immunoblots of lysates of transfected cells treated with 17-AAG. Lysates were immunoprecipitated with AR-specific antibody. The short time exposure to 17-AAG did not decrease the amount of mutant AR. There were dose-dependent changes in both Hop and p23 after treatment with 17-AAG; however, no dissociation of Hsp90 from the mutant AR complex was seen. There were no changes in the expression of Hop, p23 and Hsp90 in whole lysates in the presence of 17-AAG. (b) Densitometric analysis of Hop and p23 in the bound fractions. There was a marked increase in the amount of Hop, and a marked decrease in p23 in both wild-type and mutant AR-bound Hsp90 complexes after treatment with 17-AAG. R.S.I., relative signal intensity. (c) Comparisons of induction rate of Hop and reduction rate of p23 in the Hsp90 complexes of wild-type and mutant AR. Although there was no significant difference in the induction rate of Hop between the wild-type and mutant AR complexes, the reduction rate of p23 was significantly higher in the mutant AR complex compared with that in the wild-type complex (43.8% versus 79.0%, $P < 0.005$). Values are expressed as means \pm s.e.m. ($n = 5$). (d) Effect of 17-AAG on AR expression under the inhibition of proteasomal degradation. The mutant AR was more markedly reduced than wild-type AR after 17-AAG treatments; however, this pharmacological degradation was completely blocked by MG132 in both cases. DM, DMSO. * $P < 0.025$, ** $P < 0.005$.

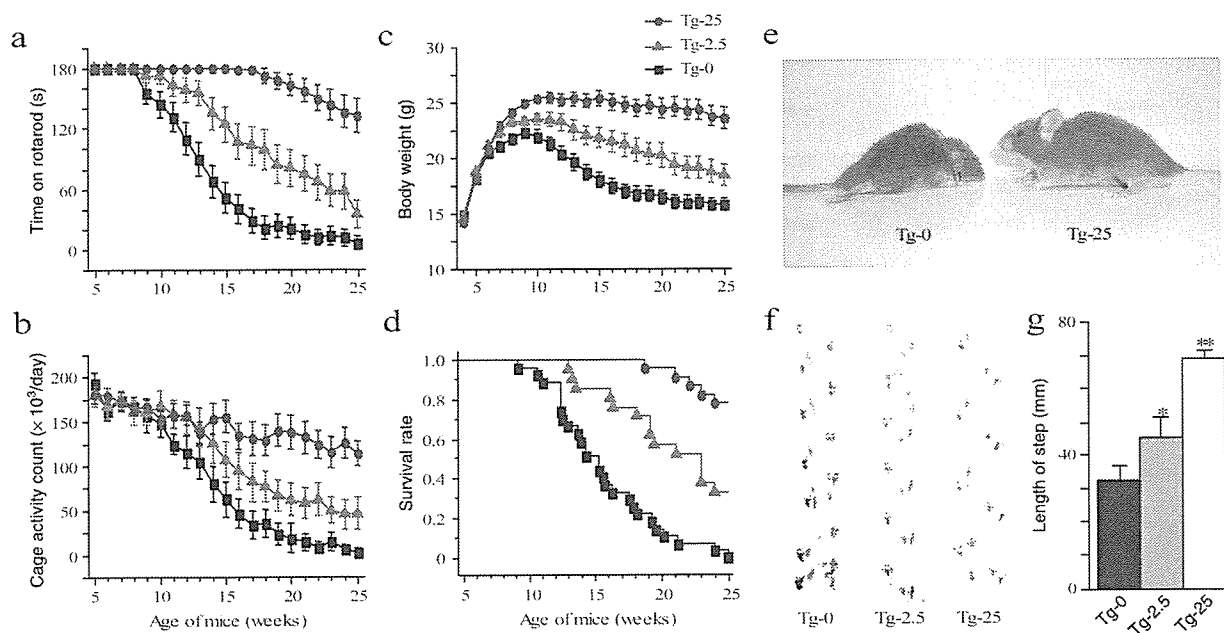


Figure 4 Effects of 17-AAG on behavioral and visible phenotypes in male AR-97Q mice. (a) Rotarod task ($n = 27$), (b) cage activity ($n = 18$), (c) body weight ($n = 27$) and (d) survival rate ($n = 27$) of Tg-0, Tg-2.5 and Tg-25 mice. All parameters were significantly different between the Tg-0 and Tg-25 ($P < 0.005$ for all parameters). A Kaplan-Meier plot shows the prolonged survival of Tg-2.5 and Tg-25 compared with Tg-0, which had all died by 25 weeks of age ($P = 0.004$, $P < 0.001$, respectively). (e) Representative photographs of a 16-week-old Tg-0 (left) shows an obvious difference in size, and illustrates muscular atrophy and kyphosis compared with an age-matched Tg-25 (right). (f) Footprints of representative 16-week-old Tg-0, Tg-2.5 and Tg-25 mice. Front paws are indicated in red and hind paws in blue. (g) The length of steps was measured in 16-week-old Tg-0, Tg-2.5 and Tg-25 mice. Each column shows an average of steps of the hind paw. Values are expressed as means \pm s.e.m. ($n = 6$). * $P < 0.025$, ** $P < 0.005$.

markedly ameliorated, and that of mice treated with the 2.5 mg/kg 17-AAG (Tg-2.5) was mildly ameliorated (Fig. 4a–d). The untreated transgenic male mice (Tg-0) showed motor impairment assessed by the rotarod task as early as 9 weeks after birth, whereas Tg-25 mice showed initial impairment only 18 weeks after birth and with less deterioration than Tg-0 mice (Fig. 4a). Tg-2.5 mice showed intermediate levels of impairment in rotarod performance (Fig. 4a). The locomotor cage activity of Tg-0 mice was also markedly decreased at 10 weeks compared with the other two groups, which showed decreases in activity at 13 (Tg-2.5) and 16 (Tg-25) weeks of age (Fig. 4b). Tg-0 mice lost weight significantly earlier and more profoundly than the Tg-2.5 ($P < 0.025$) and Tg-25 mice ($P < 0.005$; Fig. 4c). Treatment with 17-AAG also significantly prolonged the survival rate of Tg-2.5 ($P = 0.004$) and Tg-25 mice ($P < 0.001$) as compared to Tg-0 mice (Fig. 4d). 17-AAG was less effective at the dose of 2.5 mg/kg than 25 mg/kg in all parameters tested. The lines were not distinguishable in terms of body weight at birth; however, by 16 weeks, Tg-0 mice showed obvious differences in body size, muscular atrophy and kyphosis compared to Tg-25 mice (Fig. 4e). Additionally, Tg-0 mice showed motor weakness, with short steps and dragging of the legs, whereas Tg-25 mice showed almost normal ambulation (Fig. 4f,g).

When we immunohistochemically examined mouse tissues for mutant AR using the 1C2 antibody, which specifically recognizes expanded polyQ, we observed a marked reduction in 1C2-positive nuclear accumulation in the spinal motor neurons (Fig. 5a) and muscles (Fig. 5b) of Tg-25 mice compared with those of Tg-0 mice. Glial fibrillary acidic protein (GFAP)-specific antibody staining showed an apparent reduction of reactive astrogliosis in Tg-25 compared with Tg-0 mice in the spinal anterior horn (Fig. 5c). Muscle histology also showed marked amelioration of neurogenic muscle

atrophy in the AR-97Q mice treated with 17-AAG (Fig. 5d). We confirmed a significant reduction of 1C2-positive nuclear accumulation in both spinal cord ($P < 0.01$) and skeletal muscle ($P < 0.05$) by quantitative assessment (Fig. 5e). AR-24Q mice and normal littermates treated with 17-AAG showed no altered phenotypes (data not shown).

To evaluate the toxic effects of 17-AAG, we examined blood samples from 25-week-old mice treated with 25 mg/kg 17-AAG for 20 weeks. Measurements of aspartate aminotransferase, alanine aminotransferase, blood urea nitrogen and serum creatinine showed that treatment with 17-AAG resulted in neither infertility nor liver or renal dysfunction in the AR-97Q male mice at the dose of 25 mg/kg (Supplementary Fig. 2 online).

Mutant AR is preferentially degraded by 17-AAG in vivo
As the mutant AR was preferentially degraded as compared to the wild-type AR in the presence of 17-AAG in vitro, we also examined the level of AR in the SBMA mouse model. Western blot analysis of lysates of the spinal cord and muscle of AR-97Q mice showed high molecular-weight mutant AR protein complex retained in the stacking gel as well as a band of monomeric mutant AR, whereas only the band of wild-type monomeric AR was visible in tissues from the AR-24Q mice (Fig. 6a,b). Treatment with 17-AAG notably diminished both the high molecular-weight complex and the monomer of mutant AR in the spinal cord and muscle of the AR-97Q mice, but only slightly diminished the wild-type monomeric AR in AR-24Q mice (Fig. 6a,b). Treatment with 17-AAG decreased the amount of the monomeric AR in AR-97Q mice by 64.4% in the spinal cord and 45.0% in the skeletal muscle, whereas these amounts were only 25.9% and 12.5%, respectively, in AR-24Q mice (Fig. 6a,b). Thus, the reduction rate of the monomeric mutant AR was significantly higher than the wild-type

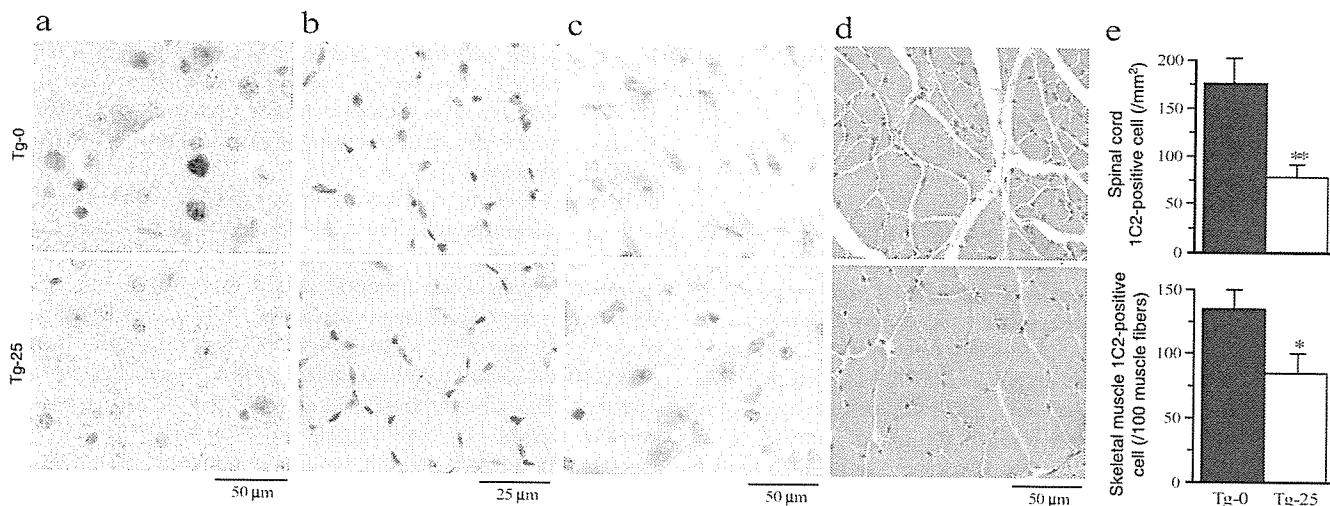


Figure 5 Effects of 17-AAG on the histopathology of male AR-97Q mice. (a,b) Immunohistochemical staining with 1C2-specific antibody showed marked differences in diffuse nuclear staining and nuclear inclusions between Tg-0 and Tg-25 mice in the spinal anterior horn and skeletal muscle, respectively. (c) Immunohistochemical staining with GFAP-specific antibody also showed an obvious reduction of reactive astrogliosis in the spinal anterior horn of mice treated with 17-AAG. (d) Hematoxylin and eosin staining of the muscle in Tg-0 mice showed obvious grouped atrophy and small angulated fibers, which were not seen in Tg-25 mice. (e) There was a significant reduction in 1C2-positive cell staining in the spinal cord ($P < 0.01$) and skeletal muscle ($P < 0.05$) in Tg-25 as compared to Tg-0 mice. Values are expressed as mean \pm s.e.m. ($n = 6$). * $P < 0.05$, ** $P < 0.01$.

AR in both spinal cord ($P < 0.001$) and skeletal muscle ($P < 0.01$; Fig. 6c). The levels of wild-type and mutant AR mRNA were similar in the respective mice treated with 17-AAG (Fig. 6d). We also performed filter-trap assays for quantitative analyses of both the large molecular aggregated and soluble forms of the mutant AR³⁶. Both forms of trapped AR-97Q protein were markedly reduced in the spinal cord and muscle of Tg-25 mice, whereas those from the AR-24Q were not (Supplementary Fig. 3 online). These observations strongly indicate that 17-AAG markedly reduces not only the monomeric mutant AR protein but also the high molecular-weight mutant AR complex, because of the preferential degradation of the mutant AR.

Western blot analysis showed that the levels of Hsp70 and Hsp40 in spinal cord were increased by 47.1% and 29.5%, respectively, and in muscle by 29.2% and 24.7%, respectively (Supplementary Fig. 4 online) after treatment with 17-AAG. These pharmacological effects of chaperone induction were statistically significant ($P < 0.05$ for all parameters), but not as marked as the 17-AAG-induced mutant AR

reduction, and were also not as pronounced as those arising from genetic manipulation in our previous study³⁶.

Hsp90 inhibitors nonspecifically activate heat shock responses through a dissociation of the heat-shock transcription factor (HSF-1) from the Hsp90 complex^{27,41}. Although the expression of

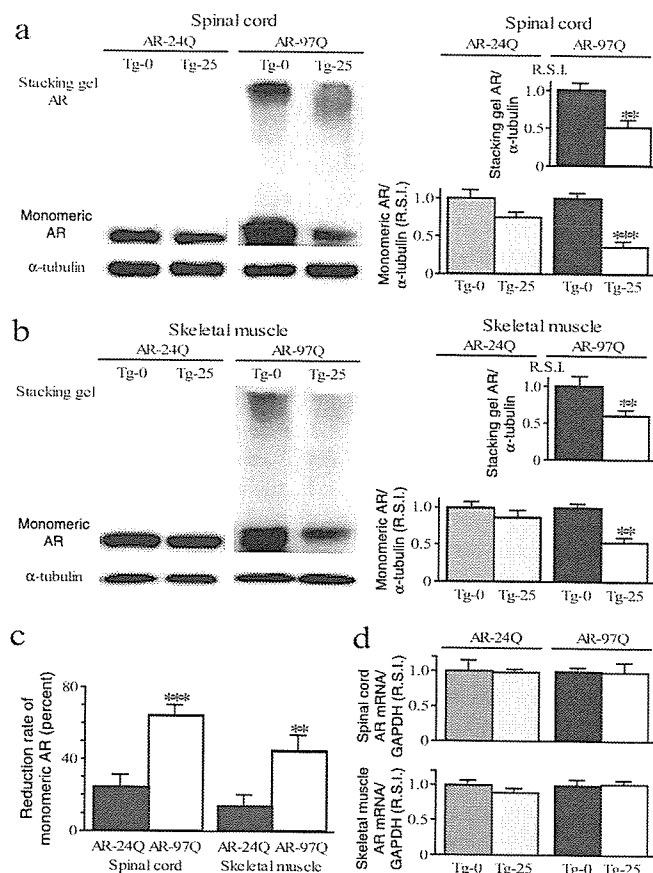


Figure 6 Effects of 17-AAG on AR expression in male AR-24Q or 97Q mice. (a,b) Western blot analysis of the spinal cord and muscle of AR-24Q and AR-97Q mice probed with AR-specific antibody. In both spinal cord and muscle of mice treated with 17-AAG, there was a significant decrease in the amount of mutant AR in the stacking gel and monomeric mutant AR in AR-97Q mice, but only slightly less monomeric wild-type AR in AR-24Q mice compared with that from untreated control mice. (c) Comparison of reduction rate of wild-type and mutant AR. Densitometric analysis showed that the 17-AAG-induced reduction of monomeric mutant AR was significantly greater than that of the wild-type monomeric AR. 17-AAG resulted in a 64.4% decline in monomeric mutant AR in the spinal cord, and a 45.0% decline in the skeletal muscle, whereas there was only a 25.9% decline in the spinal cord and a 12.5% decline in the skeletal muscle of AR-24Q mice. These results show significant differences of the reduction rate between wild-type and mutant AR in both spinal cord and skeletal muscle. Values are expressed as mean \pm s.e.m. ($n = 5$). * $P < 0.05$, ** $P < 0.01$, *** $P < 0.001$. (d) Real-time RT-PCR of wild-type and mutant AR mRNA in vivo. The expression levels of wild-type and mutant AR mRNA in transgenic mouse spinal cord and skeletal muscle were similar under 17-AAG treatments. Values are expressed as mean \pm s.e.m. ($n = 3$).

Hsp90 and HSF-1 was not altered after 17-AAG treatment, coimmunoprecipitation of HSF-1 with Hsp90 in the spinal cord and skeletal muscle was significantly reduced ($P < 0.01$ for both) after 17-AAG treatment (Supplementary Fig. 4 online), indicating that this drug induces Hsps through activation of HSF-1.

DISCUSSION

Our study showed that the polyQ-expanded mutant AR present in SBMA was preferentially degraded by treatment with 17-AAG. Elimination of mutant AR was mediated through its preferential incorporation into the Hsp90-chaperone complex, where it is then prone to proteasomal degradation. Owing to this mechanism, 17-AAG markedly ameliorated motor phenotypes of the SBMA mouse model without toxicity. Our present data from the mouse model also confirmed that 17-AAG passes through the blood-brain barrier as previously reported⁴², and that it reaches a concentration high enough to have effects in the central nervous system.

Recently, some antitumor agents have been therapeutically applied to neurodegenerative diseases^{43,44}. Most antitumor agents have some cytotoxic effects on normal cells, which must be overcome in any clinical application against neurodegeneration. Because neurodegenerative diseases generally follow a chronic progression and the medical treatment is, thus, long-standing compared to that for malignancy, the toxic side effects should be extensively suppressed. In contrast to general antitumor agents, the effects of 17-AAG have been known to have a high selectivity for tumor cells. This selectivity results from the high affinity of 17-AAG for the Hsp90 client oncoproteins when they are incorporated in the Hsp90-dependent multichaperone complex, thereby increasing their binding affinity for 17-AAG more than 100-fold¹⁹. This high selectivity of 17-AAG for the incorporated Hsp90 client protein eventually minimizes its toxic side effects and renders it very feasible for clinical applications, especially for neurodegenerative diseases. In fact, our transgenic mice were free from obvious side effects after the consecutive administration of 17-AAG for 20 weeks.

The major pharmacological effect of 17-AAG is to promote the dissociation of p23 from Hsp90 client protein complexes^{10-12,16}. In this study, we showed that the mutant AR with an expanded polyQ had a higher association with p23 than did the wild-type AR. We consider this significantly higher association between the mutant AR and p23, particularly compared with the wild-type AR, to be the essential basis for preferential degradation of the polyQ-expanded mutant AR after 17-AAG treatment. Furthermore, the increase in Hop and decrease in p23 in the mutant AR-bound Hsp90 complex after 17-AAG treatment strongly supports the view that Hsp90 complexes were shifted to the proteasome-targeting form by 17-AAG, leading to proteasomal degradation of mutant AR. Given that the increase in Hop proteins in Hsp90 complexes and the decrease in p23 were only detected after the higher concentration of 17-AAG and after a very short period of incubation, this chaperone complex shift seems to be very rapid, as has been suggested previously¹².

Hsps, particularly Hsp70, have been shown to suppress aggregate formation and cellular toxicity in a wide range of polyQ disease models^{21,36,45,46}. Geldanamycin has been considered a neuroprotective agent because of its ability to induce Hsp70 (refs. 22–24,27), and in polyQ diseases, has been proven to suppress aggregation of mutant huntingtin protein in a cultured-cell model through the induction of Hsp70 and Hsp40 (refs. 22,23). Hsp90 inhibitors have also been shown to be effective in animal models of Parkinson disease²⁴, stroke²⁷ and autoimmune encephalomyelitis²⁸. It was thought that these effects were based only on the ability of the Hsp90 inhibitors to induce Hsps. As shown in this study, however, 17-AAG induced only limited

amounts of Hsp70 and Hsp40 *in vivo*. Furthermore, our results suggest that the pathway for mutant AR degradation by 17-AAG through the Hsp90-client protein complex system is predominant. 17-AAG is expected to exert the most effective therapeutic potential for diseases in which the disease-causing protein belongs to the Hsp90 client protein family.

Mutant p53, which is present in nearly half of all malignancies and is an Hsp90 client protein, shows a much higher sensitivity to Hsp90 inhibitors than does wild-type p53 (ref. 47), just as AR, in its polyQ-expanded mutant form, acquired higher sensitivity to the Hsp90 inhibitor. In the case of neurodegenerative diseases, phosphorylated tau would be one of the target proteins of Hsp90 inhibitors, because geldanamycin substantially reduces the total amount of phosphorylated tau^{25,26}, and also inhibits tau aggregation²⁵. According to these previous reports, our data suggest that 17-AAG would also be a candidate for a therapeutic approach to a wide range of tauopathies. The successful application of 17-AAG to polyQ diseases other than SBMA remains to be seen. But, as a previous report showed, the blockage of pathogenic gene expression could reversibly reduce nuclear inclusions and reactive gliosis in a mouse model of Huntington disease by self-cleaning functions⁴⁸. Indeed, one therapeutic approach, which directly reduced abnormal protein using RNA interference, proved to be beneficial in a mouse model of SCA1 (ref. 49). There is no doubt that the reduction of disease-causing protein would be beneficial in polyQ diseases. Therefore, once it is proven that the disease-causing proteins belong to the Hsp90 client protein family and have high affinities to Hsp90 inhibitors, 17-AAG is expected to preferentially degrade the expanded polyQ-containing disease proteins and, thus, would be a good candidate for clinical therapeutics.

In conclusion, we have shown the efficacy and safety of 17-AAG in a model mouse of SBMA, a neurodegenerative disease, and considerably extended the therapeutic application of 17-AAG beyond oncological diseases. In addition, we have documented the differential degradation efficacy of a polyQ-expanded mutant protein compared with its wild-type form. This strategy is apparently different from the previous strategy for polyQ diseases, which unavoidably allowed abnormal protein to remain and placed much value mainly on the inhibition of protein aggregation. 17-AAG, directly reducing disease-causing protein itself, presents a new therapeutic avenue for SBMA, and has potentially widespread application for other neurodegenerative diseases.

METHODS

DNA transfection. We constructed full-length ARs by subcloning AR inserts derived from pSP64-AR24 or pSP64-AR97 (ref. 46) into the pCR3.1 mammalian expression vector (Invitrogen). We plated SH-SY5Y cells in 6-cm dishes and transfected each dish with 8 ng of the vector containing AR24 or AR97 using Lipofectamine 2000 (Invitrogen) according to the manufacturer's instructions. We cultured the cells for 48 h. In this culture system, we detected a band of monomeric mutant AR in the separating gel, but could hardly detect the high molecular-weight mutant AR protein complex, which was retained in the stacking gel.

Neurological and behavioral assessment of SBMA model mice. We generated and maintained the AR-24Q and AR-97Q mice as previously described³⁵ (Supplementary Methods online). All animal experiments were performed in accordance with the National Institutes of Health Guide for the Care and Use of Laboratory Animals and under the approval of the Nagoya University Animal Experiment Committee. We performed the mouse rotarod task and cage activity as described previously³⁵. The investigators in the behavioral assessment were blinded to the treatments.

Therapeutic agents and protocol for administration. We obtained 17-AAG, also known as NSC 330507, from the Regulatory Affairs Branch, Division of



Cancer Treatment and Diagnosis, National Cancer Institute and Kosan Biosciences. For cultured-cell models, we diluted a 1.8 mM stock solution of 17-AAG in DMSO into fresh medium to give final concentrations of 18–360 nM. In the cycloheximide study, we treated cells for 48 h with 17-AAG in the presence of 5 ng/ml cycloheximide (Sigma). To show pharmacological changes in the AR-Hsp90 complex, we exposed cultured cells for 30 min to 17-AAG at concentrations of 0.36, 3.6 and 36 nM 48 h after transfection. In the proteasome-inhibitory study, we exposed cultured cells for 6 h to 36 nM 17-AAG, and 5, 10 and 20 nM MG132 (Sigma) beginning 48 h after transfection.

For mouse models, we stored 50 mg/ml stock solutions of 17-AAG dissolved in DMSO at -20°C . We began 17-AAG treatments when mice attained the age of 5 weeks, and continued them until mice were 25 weeks old. Normal male littermates, AR-24Q mice and AR-97Q mice received 50 ml intraperitoneal injections of 2.5 or 25 mg/kg 17-AAG three times a week on alternate days; control mice received DMSO alone.

Protein expression analysis. We lysed cells in CelLytic-M Mammalian Cell Lysis/Extraction Reagent (Sigma) and centrifuged them at 15,000g for 15 min at 4 $^{\circ}\text{C}$. We homogenized the tissues from 16-week-old mice in CelLytic-M (Sigma) and centrifuged them at 2,500g for 15 min at 4 $^{\circ}\text{C}$. Primary antibodies were as follows: AR-specific antibody (N-20 or H280; Santa Cruz); Hsp70-specific antibody (SPA-810; Stressgen); Hsp40-specific antibody (SPA-400; Stressgen); Hsp90-specific antibody (SPA-835; Stressgen); Hop-specific antibody (SRA-1500; Stressgen); p23-specific antibody (MA3-414; Affinity Bio-Reagents); HSF-1-specific antibody (SPA-901; Stressgen); p85-specific antibody (Upstate); and α -tubulin-specific antibody (T9026; Sigma). We used the LAS-3000 imaging system to produce digital images and to quantify band intensities, which we then analyzed with Image Gauge software version 4.22 (Fujifilm). Densitometric values of AR, Hsp70, Hsp40 and Hsp90 were normalized to those of endogenous p85 or α -tubulin. Relative signal intensity (R.S.I.) was computed as the signal intensity of each sample divided by that of DMSO-treated cells or DMSO-treated mice.

We performed immunoprecipitation from cultured cells using 300 ng total protein lysate from cells, 10 ml Protein G Sepharose (Amersham) and 5 ml AR-specific antibody (N-20). For experiments involving coprecipitation of AR, we lysed cells in molybdate-containing lysis buffer^{11,12,16}. Immunoprecipitation from mouse tissues was performed using 1 mg total protein lysed in CelLytic-M (Sigma). R.S.I. was computed as the signal intensity of each sample divided by that of AR-24Q cells, DMSO-treated cells or DMSO-treated mice.

Pulse-chase labeling assay. We transfected cells as described above, starved them for 1 h, and then labeled them for 1 h with 150 nCi of Redivue Pro-Mix L-[³⁵S] in vitro cell-labeling mix (Amersham) per milliliter. We chased the cells for the indicated time intervals in complete medium with DMSO or 360 nM 17-AAG. We performed immunoprecipitation using equivalent amounts of protein lysates as described above, and analyzed by phosphorimaging (Typhoon 8600 phosphorimager; Amersham) and Image Gauge software, version 4.22 (Fujifilm).

Quantitative real-time RT-PCR. We determined the levels of AR mRNA by real-time Taqman PCR by the iCycler system (Bio-Rad) as previously described²⁰. R.S.I. was computed as the signal intensity of each sample divided by that of DMSO-treated cells or DMSO-treated control mice.

Immunohistochemistry and histopathology. We prepared tissues as previously described^{35–38}. We incubated the tissue sections with expanded polyQ-specific antibody (1:10,000, 1C2; Chemicon) and GFAP-specific antibody (1:1,000, Boehringer Mannheim). We air-dried 6 mm-thick paraffin-embedded sections of the gastrocnemius muscles and stained them with hematoxylin and eosin. For quantification of 1C2-positive cells, we counted the number of 1C2-positive cells of the thoracic spinal cord and gastrocnemius muscle in each individual mouse as previously described³⁶.

Statistical analysis. We analyzed data by unpaired t-tests and Kaplan-Meier and log-rank tests for survival rate using Statview software version 5 (HULINKS). We examined statistical significance of the drug-dose dependency by the Williams test for multiple comparisons using Microsoft Excel 2004 (Microsoft).

Accession codes. BIND identifiers (<http://bind.ca>): 316918.

Note: Supplementary information is available on the Nature Medicine website.

ACKNOWLEDGMENTS

We thank National Cancer Institute and Kosan Biosciences for kindly providing 17-AAG. This work was supported by a Center of Excellence (COE) grant from the Ministry of Education, Culture, Sports, Science and Technology, Japan, and by grants from the Ministry of Health, Labor and Welfare, Japan.

COMPETING INTERESTS STATEMENT

The authors declare that they have no competing financial interests.

Published online at <http://www.nature.com/naturemedicine/>

Reprints and permissions information is available online at <http://npj.nature.com/reprintsandpermissions/>

- Pratt, W.B. & Toft, D.O. Regulation of signaling protein function and trafficking by the hsp90/hsp70-based chaperone machinery. *Exp. Biol. Med.* (Maywood) 228, 111–133 (2003).
- Neckers, L., Schulte, T.W. & Minnaugh, E. Geldanamycin as a potential anti-cancer agent: its molecular target and biochemical activity. *Invest. New Drugs* 17, 361–373 (1999).
- Supko, J.G., Hickman, R.L., Grever, M.R. & Malspeis, L. Preclinical pharmacologic evaluation of geldanamycin as an antitumor agent. *Cancer Chemother. Pharmacol.* 36, 305–315 (1995).
- Schulte, T.W. & Neckers, L.M. The benzoquinone ansamycin 17-allylamino-17-demethoxygeldanamycin binds to HSP90 and shares important biologic activities with geldanamycin. *Cancer Chemother. Pharmacol.* 42, 273–279 (1998).
- Page, J. et al. Comparison of geldanamycin (NSC-122750) and 17-allylamino-geldanamycin (NSC-330507D) toxicity in rats. *Proc. Am. Assoc. Cancer Res.* 38, 308 (1997).
- Sullivan, W. et al. Nucleotides and two functional states of hsp90. *J. Biol. Chem.* 272, 8007–8012 (1997).
- Bagatell, R. et al. Destabilization of steroid receptors by heat shock protein 90-binding drugs: a ligand-independent approach to hormonal therapy of breast cancer. *Clin. Cancer Res.* 7, 2076–2084 (2001).
- Neckers, L. Heat shock protein 90 inhibition by 17-allylamino-17-demethoxygeldanamycin: a novel therapeutic approach for treating hormone-refractory prostate cancer. *Clin. Cancer Res.* 8, 962–966 (2002).
- Felts, S.J. & Toft, D.O. p23, a simple protein with complex activities. *Cell Stress Chaperones* 8, 108–113 (2003).
- Johnson, J.L. & Toft, D.O. Binding of p23 and hsp90 during assembly with the progesterone receptor. *Mol. Endocrinol.* 9, 670–678 (1995).
- Smith, D.F. et al. Progesterone receptor structure and function altered by geldanamycin, an hsp90-binding agent. *Mol. Cell. Biol.* 15, 6804–6812 (1995).
- Whitesell, L. & Cook, P. Stable and specific binding of heat shock protein 90 by geldanamycin disrupts glucocorticoid receptor function in intact cells. *Mol. Endocrinol.* 10, 705–712 (1996).
- Schneider, C. et al. Pharmacologic shifting of a balance between protein refolding and degradation mediated by Hsp90. *Proc. Natl. Acad. Sci. USA* 93, 14536–14541 (1996).
- Solit, D.B. et al. 17-Allylamino-17-demethoxygeldanamycin induces the degradation of androgen receptor and HER-2/neu and inhibits the growth of prostate cancer xenografts. *Clin. Cancer Res.* 8, 986–993 (2002).
- Vánaja, D.K., Mitchell, S.H., Toft, D.O. & Young, C.Y. Effect of geldanamycin on androgen receptor function and stability. *Cell Stress Chaperones* 7, 55–64 (2002).
- Beliakoff, J. et al. Hormone-refractory breast cancer remains sensitive to the antitumor activity of heat shock protein 90 inhibitors. *Clin. Cancer Res.* 9, 4961–4971 (2003).
- Bonvini, P., Dalla Rosa, H., Vignes, N. & Rosolen, A. Ubiquitination and proteasomal degradation of nucleophosmin-anaplastic lymphoma kinase induced by 17-allylamino-demethoxygeldanamycin: role of the co-chaperone carboxyl heat shock protein 70-interacting protein. *Cancer Res.* 64, 3256–3264 (2004).
- Minnaugh, E.G., Chavany, C. & Neckers, L. Polyubiquitination and proteasomal degradation of the p185c-erbB-2 receptor protein-tyrosine kinase induced by geldanamycin. *J. Biol. Chem.* 271, 22796–22801 (1996).
- Kamal, A. et al. A high-affinity conformation of Hsp90 confers tumour selectivity on Hsp90 inhibitors. *Nature* 425, 407–410 (2003).
- Whitesell, L., Bagatell, R. & Falsey, R. The stress response: implications for the clinical development of hsp90 inhibitors. *Curr. Cancer Drug Targets* 3, 349–358 (2003).
- Michowski, P.J. & Wacker, J.L. Modulation of neurodegeneration by molecular chaperones. *Nat. Rev. Neurosci.* 6, 11–22 (2005).
- Sittler, A. et al. Geldanamycin activates a heat shock response and inhibits huntingtin aggregation in a cell culture model of Huntington's disease. *Hum. Mol. Genet.* 10, 1307–1315 (2001).
- Hay, D.G. et al. Progressive decrease in chaperone protein levels in a mouse model of Huntington's disease and induction of stress proteins as a therapeutic approach. *Hum. Mol. Genet.* 13, 1389–1405 (2004).
- Auluck, P.K. & Bonini, N.M. Pharmacological prevention of Parkinson disease in *Drosophila*. *Nat. Med.* 8, 1185–1186 (2002).
- Dou, F. et al. Chaperones increase association of tau protein with microtubules. *Proc. Natl. Acad. Sci. USA* 100, 721–726 (2003).



26. Petrucelli, L. et al. CHIP and Hsp70 regulate tau ubiquitination, degradation and aggregation. *Hum. Mol. Genet.* 13, 703–714 (2004).
27. Lu, A., Ran, R., Parmentier-Batteur, S., Nee, A. & Sharp, F.R. Geldanamycin induces heat shock proteins in brain and protects against focal cerebral ischemia. *J. Neurochem.* 81, 355–364 (2002).
28. Murphy, P. et al. Suppressing effects of ansamycins on inducible nitric oxide synthase expression and the development of experimental autoimmune encephalomyelitis. *J. Neurosci. Res.* 67, 461–470 (2002).
29. La Spada, A.R., Wilson, E.M., Lubahn, D.B., Harding, A.E. & Fischbeck, K.H. Androgen receptor gene mutations in Xlinked spinal and bulbar muscular atrophy. *Nature* 352, 77–79 (1991).
30. Sobue, G. et al. Xlinked recessive bulbospinal neuronopathy: A clinicopathological study. *Brain* 112, 209–232 (1989).
31. Zoghbi, H.Y. & Orr, H.T. Glutamine repeats and neurodegeneration. *Annu. Rev. Neurosci.* 23, 217–247 (2000).
32. Tanaka, F. et al. Founder effect in spinal and bulbar muscular atrophy (SBMA). *Hum. Mol. Genet.* 5, 1253–1257 (1996).
33. Doyu, M. et al. Severity of Xlinked recessive bulbospinal neuronopathy correlates with size of the tandem CAG repeat in androgen receptor gene. *Ann. Neurol.* 32, 707–710 (1992).
34. Adachi, H. et al. Widespread nuclear and cytoplasmic accumulation of mutant androgen receptor in SBMA patients. *Brain* 128, 659–670 (2005).
35. Katsuno, M. et al. Testosterone reduction prevents phenotypic expression in a transgenic mouse model of spinal and bulbar muscular atrophy. *Neuron* 35, 843–854 (2002).
36. Adachi, H. et al. Heat shock protein 70 chaperone overexpression ameliorates phenotypes of the spinal and bulbar muscular atrophy transgenic mouse model by reducing nuclear-localized mutant androgen receptor protein. *J. Neurosci.* 23, 2203–2211 (2003).
37. Katsuno, M. et al. Leuprorelin rescues polyglutamine-dependent phenotypes in a transgenic mouse model of spinal and bulbar muscular atrophy. *Nat. Med.* 9, 768–773 (2003).
38. Minamiyama, M. et al. Sodium butyrate ameliorates phenotypic expression in a transgenic mouse model of spinal and bulbar muscular atrophy. *Hum. Mol. Genet.* 13, 1183–1192 (2004).
39. Bailey, C.K., Andriola, I.F., Kampinga, H.H. & Merry, D.E. Molecular chaperones enhance the degradation of expanded polyglutamine repeat androgen receptor in a cellular model of spinal and bulbar muscular atrophy. *Hum. Mol. Genet.* 11, 515–523 (2002).
40. Lieberman, A.P., Hamison, G., Strand, A.D., Olson, J.M. & Fischbeck, K.H. Altered transcriptional regulation in cells expressing the expanded polyglutamine androgen receptor. *Hum. Mol. Genet.* 11, 1967–1976 (2002).
41. Zou, J., Guo, Y., Guettouche, T., Smith, D.F. & Voellmy, R. Repression of heat shock transcription factor HSF1 activation by HSP90 (HSP90 complex) that forms a stress-sensitive complex with HSF1. *Cell* 94, 471–480 (1998).
42. Egorin, M.J. et al. Plasma pharmacokinetics and tissue distribution of 17-(allylamino)-17-demethoxygeldanamycin (NSC 330507) in CD2F1 mice. *Cancer Chemother. Pharmacol.* 47, 291–302 (2001).
43. Ravikumar, B. et al. Inhibition of mTOR induces autophagy and reduces toxicity of polyglutamine expansions in fly and mouse models of Huntington disease. *Nat. Genet.* 36, 585–595 (2004).
44. Ferrante, R.J. et al. Chemotherapy for the brain: the antitumor antibiotic mithramycin prolongs survival in a mouse model of Huntington's disease. *J. Neurosci.* 24, 10335–10342 (2004).
45. Cummings, C.J. et al. Chaperone suppression of aggregation and altered subcellular proteasome localization imply protein misfolding in SCA1. *Nat. Genet.* 19, 148–154 (1998).
46. Kobayashi, Y. et al. Chaperones Hsp70 and Hsp40 suppress aggregate formation and apoptosis in cultured neuronal cells expressing truncated androgen receptor protein with expanded polyglutamine tract. *J. Biol. Chem.* 275, 8772–8778 (2000).
47. Blagosklonny, M.V., Toretsky, J., Bohlen, S. & Neckers, L. Mutant conformation of p53 translated in vitro or in vivo requires functional HSP90. *Proc. Natl. Acad. Sci. USA* 93, 8379–8383 (1996).
48. Yamamoto, A., Lucas, J.J. & Hen, R. Reversal of neuropathology and motor dysfunction in a conditional model of Huntington's disease. *Cell* 101, 57–66 (2000).
49. Xia, H. et al. RNAi suppresses polyglutamine-induced neurodegeneration in a model of spinocerebellar ataxia. *Nat. Med.* 10, 816–820 (2004).
50. Ishigaki, S. et al. X-linked inhibitor of apoptosis protein is involved in mutant SOD1-mediated neuronal degeneration. *J. Neurochem.* 82, 576–584 (2002).



Underediting of GluR2 mRNA, a neuronal death inducing molecular change in sporadic ALS, does not occur in motor neurons in ALS1 or SBMA

Yukio Kawahara^{a,1}, Hui Sun^a, Kyoko Ito^a, Takuto Hideyama^a,
Masashi Aoki^b, Gen Sobue^c, Shoji Tsuji^a, Shin Kwak^{a,*}

^aDepartment of Neurology, Graduate School of Medicine, The University of Tokyo,
7-3-1 Hongo, Bunkyo-ku, Tokyo 113-8655, Japan

^bDepartment of Neurology, Tohoku University Graduate School of Medicine, Sendai, Japan

^cDepartment of Neurology, Nagoya University Graduate School of Medicine, Nagoya, Japan

Received 7 July 2005; accepted 13 September 2005

Available online 12 October 2005

Abstract

Deficient RNA editing of the AMPA receptor subunit GluR2 at the Q/R site is a primary cause of neuronal death and recently has been reported to be a tightly linked etiological cause of motor neuron death in sporadic amyotrophic lateral sclerosis (ALS). We quantified the RNA editing efficiency of the GluR2 Q/R site in single motor neurons of rats transgenic for mutant human Cu/Zn-superoxide dismutase (SOD1) as well as patients with spinal and bulbar muscular atrophy (SBMA), and found that GluR2 mRNA was completely edited in all the motor neurons examined. It seems likely that the death cascade is different among the dying motor neurons in sporadic ALS, familial ALS with mutant SOD1 and SBMA.
2005 Elsevier Ireland Ltd and the Japan Neuroscience Society. All rights reserved.

Keywords: ALS; SOD1; Spinal and bulbar muscular atrophy; Motor neuron; RNA editing; GluR2; AMPA receptor; Neuronal death

1. Introduction

Amyotrophic lateral sclerosis (ALS) is a progressive neurodegenerative disease with selective loss of both upper and lower motor neurons, and familial cases are rare. The etiology of sporadic ALS remains elusive but recently deficient RNA editing of AMPA receptor subunit GluR2 at the Q/R site is reported in motor neurons in ALS that occurs in a disease-specific and motor neuron-selective manner (Kawahara et al., 2004; Kwak and Kawahara, 2005). Moreover, underediting of the GluR2 Q/R site greatly increases the Ca²⁺ permeability of AMPA receptors (Hume et al., 1991; Verdoorn et al., 1991; Burnashev et al., 1992), which may cause neuronal death due to increased Ca²⁺ influx through the receptor channel, hence mice with RNA editing deficiencies at the GluR2 Q/R site die young (Brusa et al., 1995) and mice transgenic for an artificial Ca²⁺-

permeable GluR2 develop motor neuron disease 12 months after birth (Kuner et al., 2005). Such evidence lends strong support to the close relevance of deficient RNA editing of the GluR2 at the Q/R site to death of motor neurons in sporadic ALS. However, although we and other researchers have demonstrated that dying neurons in several neurodegenerative diseases exhibit edited GluR2 (Kwak and Kawahara, 2005), it has not yet been demonstrated whether the underediting of GluR2 occurs in dying motor neurons in motor neuron diseases other than ALS. Such investigation is of particular importance since it will help clarify whether the molecular mechanism of motor neurons death is common among various subtypes of motor neurons.

ALS associated with the SOD1 mutation (ALS1) is the most frequent familial ALS (Rosen et al., 1993), and mutated human SOD1 transgenic animals have been studied extensively as a disease model of ALS1, yet the etiology of neuronal death in the animals has not been elucidated. Another example of non-ALS motor neuron disease is spinal and bulbar muscular atrophy (SBMA), which predominantly affects lower motor neurons with a relatively slow clinical course. Since the CAG

* Corresponding author. Tel.: +81 3 5800 8672; fax: +81 3 5800 6548.

E-mail address: kwak-tyk@umin.ac.jp (S. Kwak).

¹ Present address: The Wistar Institute, Philadelphia, PA, USA.